

Risk-Sensitive Reinforcement Learning with Exponential Criteria

Erfaun Noorani

ENOORANI@UMD.EDU

*Department of Electrical and Computer Engineering & Institute for Systems Research
University of Maryland, College Park*

Christos N. Mavridis

MAVRIDIS@KTH.SE

*Division of Decision and Control Systems, School of Electrical Engineering and Computer Science,
KTH Royal Institute of Technology, Stockholm.*

John S. Baras

BARAS@UMD.EDU

*Department of Electrical and Computer Engineering & Institute for Systems Research
University of Maryland, College Park*

Abstract

While reinforcement learning has shown experimental success in a number of applications, it is known to be sensitive to noise and perturbations in the parameters of the system, leading to high variance in the total reward amongst different episodes on slightly different environments. To introduce robustness, as well as sample efficiency, risk-sensitive reinforcement learning methods are being thoroughly studied. In this work, we provide a definition of robust reinforcement learning policies and formulate a risk-sensitive reinforcement learning problem to approximate them, by solving an optimization problem with respect to a modified objective based on exponential criteria. In particular, we study a model-free risk-sensitive variation of the widely-used Monte Carlo Policy Gradient algorithm, and introduce a novel risk-sensitive online Actor-Critic algorithm based on solving a multiplicative Bellman equation using stochastic approximation updates. Analytical results suggest that the use of exponential criteria generalizes commonly used ad-hoc regularization approaches, improves sample efficiency, and introduces robustness with respect to perturbations in the model parameters and the environment. The implementation, performance, and robustness properties of the proposed methods are evaluated in simulated experiments.

1. Introduction

In stochastic decision systems, where uncertainty leads to risk (variability) in a desired performance metric, solving a stochastic optimal control task (viz., reinforcement learning applications) by optimizing a risk-neutral objective, often leads to control policies that might perform poorly, especially in real-world applications. This is due to the fact that risk-neutral objectives typically consist of a long-run expectation of the desired metric (average performance) which have been shown to be non-robust to noise and model uncertainties (Sutton & Barto, 2018). This phenomenon is observed in widely-used Reinforcement Learning (RL) algorithms, such as Actor-Critic methods, which are often unable to maintain their performance under slight variations in the environment at the testing time. Figure 1 shows the training and testing performance of an Actor-Critic agent in an inverted pendulum problem (see Section 5.2) with perturbed model parameters. While training is conducted with a given pole length, the performance of the trained agent is evaluated in a set of environments

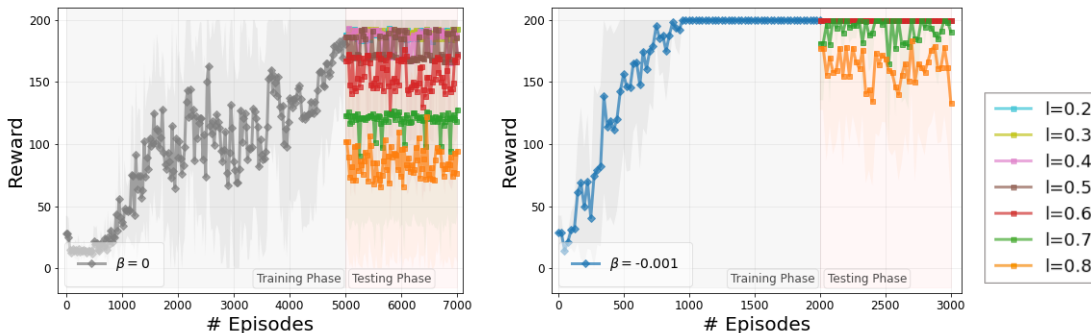


Figure 1: Generalization performance with respect to perturbations in the model parameters. Risk-neutral and risk-sensitive actor-critic reinforcement learning algorithms have been trained in the Cart-Pole environment with pole length $l = 0.5$, and tested for different pole length values $l \in [0.2, 0.8]$. Average reward and 90% confidence intervals over a running window of 10 episodes are depicted.

with different pole lengths. It is clear that, in the risk-neutral case, the change in the pole length results in significant performance degradation. To mitigate such issues, risk-sensitive RL investigates alternative optimization approaches, e.g., by incorporating constraints and alternative objective functions to induce robustness with respect to variations and uncertainties of the environment (Moos, Hansel, Abdulsamad, Stark, Clever, & Peters, 2022; Osogami, 2012; Noorani & Baras, 2021a).

Related work

Robustness has been studied extensively in optimization and optimal control (Hansen & Sargent, 2011). In reinforcement learning problems, where uncertainties in the system demand that distributional information is taken into account, robustness is associated with a stochastic optimization problem of the form:

$$\max_{\pi \in \Pi} \inf_{\rho \in \Psi} \mathbb{E}_{x \sim \pi, \zeta \sim \rho} [\mathbf{R}(x, \zeta)],$$

where $x \in X$ are the design parameters with distribution $\pi \in \Pi$, $\zeta \in Z$ is a random vector with distribution $\rho \in \Psi$ representing uncertain system parameters, and $\mathbf{R} : X \times Z \rightarrow [0, \infty)$ is an objective (reward) function to be maximized. Here the system’s sensitivity to maximum uncertainty (e.g., noise, disturbances) is maximized (Scarf, 1957). This problem is closely related to mini-max games (Shapley, 1953; Basar & Bernhard, 2008; James & Baras, 1995).

A number of risk-sensitive reinforcement learning approaches have been studied in recent years; from constructing constraint stochastic optimization problems (Paternain, Chamon, Calvo-Fullana, & Ribeiro, 2019; Delage & Mannor, 2010; Abdullah, Ren, Ammar, Milenkovic, Luo, Zhang, & Wang, 2019) or approximately solving mini-max optimization problems (Tamar, Xu, & Mannor, 2013), to investigate different statistical measures of the objective function (Pan, Seita, Gao, & Canny, 2019; Dotan Di Castro & Mannor, 2012; Prashanth, 2014; Tamar, 2015; Liu, Liu, & Xiao, 2018; Nass, Belousov, & Peters, 2019; Greenberg, Chow, Ghavamzadeh, & Mannor, 2022; Reddy, Saha, Tamilselvam, Agrawal,

& Dayama, 2019). The latter approach often yields to more favorable algorithmic implementations, since the computational problems associated with constraint optimization, and the convergence problems associated with the existence of multiple Nash equilibria are avoided. In particular, the algorithms in (Chow & Ghavamzadeh, 2014; Prashanth, 2014; Tamar, 2015; Pinto, Davidson, Sukthankar, & Gupta, 2017) use the conditional value at risk for policy search and the algorithms in (Pan et al., 2019; Dotan Di Castro & Mannor, 2012; Liu et al., 2018; Eysenbach & Levine, 2021) use variance as the desired risk measure. Along the same directions, risk-sensitive algorithms have been developed based on postulated regularized objectives, such as Kullback-Leibler (KL) regularization (Todorov, 2007; Galashov, Jayakumar, Hasenclever, Tirumala, Schwarz, Desjardins, Czarnecki, Teh, Pascanu, & Heess, 2019) or entropy regularization (Williams & Peng, 1991; Ziebart, Maas, Bagnell, & Dey, 2008; Haarnoja, Tang, Abbeel, & Levine, 2017; Haarnoja, Zhou, Abbeel, & Levine, 2018; Fei, Yang, Chen, Wang, & Xie, 2020), leading to policy search methods, such as PPO (Schulman, Wolski, Dhariwal, Radford, & Klimov, 2017), TRPO (Schulman, Levine, Abbeel, Jordan, & Moritz, 2015) and MPO (Abdolmaleki, Springenberg, Tassa, Munos, Heess, & Riedmiller, 2018).

Although these are ad-hoc approaches developed by experimental observations, there is a duality connection between KL- and entropy-regularized objectives and entropic risk measures (Borkar, 2010; Osogami, 2012; Nass et al., 2019; Noorani & Baras, 2021b), associated with exponential criteria of the form:

$$\max_{\pi \in \Pi} \frac{1}{\beta} \mathbb{E}_{x \sim \pi} [\exp(\beta R(x))].$$

In addition to this connection, exponential criteria are well-understood in the context of risk-sensitive control (Jacobson, 1973; James & Baras, 1995; Noorani & Baras, 2022), and can lead to appealing algorithmic implementations (Noorani & Baras, 2021a).

Contribution

In this work, we study the effect of exponential criteria on the robustness of the learned policy of a reinforcement learning agent. In particular, we

- formulate the risk-sensitive reinforcement learning problem as an optimization problem with a modified objective using exponential criteria and show its connection to KL-regularized RL methods (Section 2.3);
- provide a definition of robustness for RL policies and show that the use of exponential criteria results in robust RL policies with given probability bounds on the observed cumulative rewards in the form of concentration inequalities (Section 2.4);
- provide new analytic results for the implementation of the risk-sensitive REINFORCE algorithm based on exponential criteria introduced in (Noorani & Baras, 2021a) regarding the update rule and the convergence of the parameters (Section 3);
- develop a risk-sensitive online actor-critic algorithm, by solving the risk-sensitive multiplicative Bellman equation with stochastic approximation updates (Section 4); and

- quantify the robustness of the proposed methods in terms of the Conditional Value at Risk (CVaR) values of the total reward in simulated experiments under model parameter perturbations (Section 5).

Our experimental results support our theoretical analysis and suggest that the proposed problem formulation using exponential criteria is suitable for risk-sensitive reinforcement learning. The proposed risk-sensitive RL methods inherit computational and convergence properties of widely-used RL algorithms, can accelerate the learning process, and can reduce the variance of the learned policies under model uncertainty, resulting in policies that show enhanced robustness with respect to environmental and model perturbations.

2. Risk-Sensitive Reinforcement Learning with Exponential Criteria

In this section, we formulate the problem of risk-sensitive reinforcement learning and show its connection to exponential criteria. We provide an explicit definition of robustness and risk-sensitivity, and show that the use of exponential criteria is associated with a min-max optimization problem that results in robust RL policies with known concentration bounds on the observed rewards under perturbations of the agent’s environment.

2.1 Reinforcement Learning Preliminaries

The RL problem is typically modeled using a Markov Decision Process (MDP) which is represented by a tuple $\mathcal{M}=(\mathcal{S}, \mathcal{A}, \mathbf{p}_0, \mathbf{P}, r, \gamma)$, where \mathcal{S} and \mathcal{A} are, respectively, the state and action spaces (may each be discrete or continuous). The probability distribution \mathbf{p}_0 is the initial state distribution, prescribing a probability on the starting state. The kernel $\mathbf{P} : \mathcal{S} \times \mathcal{A} \rightarrow \Delta(\mathcal{S})$ is the transition kernel (unknown to the agent), where $\Delta(\mathcal{S})$ denotes the space of probability distributions on \mathcal{S} . The function $r : \mathcal{S} \times \mathcal{A} \rightarrow \mathbb{R}$ is the reward function; and $\gamma \in [0, 1)$ is a discounting factor. The behavior of an RL agent is determined by its policy. Here, we consider randomized policies.

A (randomized) policy $\pi(\cdot|s) \in \Pi$ is a probability distribution over the action space given the state, which prescribes the probability of taking an action $\mathbf{a} \in \mathcal{A}$ when in state s . Stochastic policies are smooth and continuous functions and therefore are more suitable for gradient-based methods. At each time-step t , the agent perceives the state of the environment s_t , and executes an action \mathbf{a}_t according to its policy, a differentiable parametrized policy (e.g., a Neural Network), $\pi(\cdot|s_t; \theta)$ where $\theta \in \mathbb{R}^d$ is a vector of parameters. Then, the system transitions to a successor state s_{t+1} according to transition probability $\mathbf{p}(s_{t+1}|s_t, \mathbf{a}_t)$ (unknown to the agent) and the agent receives a reward $r_t := r(s_t, \mathbf{a}_t)$. By following policy π , the agent generates trajectory $\tau(\pi)$ (a sequence of states and actions). The agent’s policy and the system transition probabilities induce a trajectory distribution, a probability distribution $\rho_\theta \in \Psi$ over the possible trajectories \mathcal{T} , given by

$$\rho_\theta(\tau) = \mathbf{p}_0 \prod_{t=0}^{|\tau|-1} \pi(\mathbf{a}_t|s_t; \theta) \mathbf{p}(s_{t+1}|s_t, \mathbf{a}_t). \quad (1)$$

The trajectory distribution is generated by following a policy parameterized with θ in an environment with transition kernel \mathbf{P} .

The RL agent aims to find a policy that maximizes the sum of rewards over a time period, called episode. Since the observed rewards r_t are random variables, in risk-neutral RL, the typical objective is to optimize for the expected (discounted) cumulative reward:

$$\max_{\theta} J(\theta) := \mathbb{E}_{\tau \sim \rho_{\theta}} [\mathbf{R}(\tau)], \quad (2)$$

where

$$\mathbf{R}(\tau) = \sum_{t=0}^{|\tau|-1} \gamma^t r(s_t, \mathbf{a}_t) \quad (3)$$

is the trajectory’s (γ -discounted) total reward. The expectation is taken with respect to the trajectory distribution. That is, the expectation is taken over the space of trajectories \mathcal{T} generated by following the policy, i.e., $s_0 \sim p_0$, $\mathbf{a}_t \sim \pi(\cdot | s_t; \theta)$ and $s_{t+1} \sim p(\cdot | s_t, \mathbf{a}_t)$. In the rest of this manuscript, we will use the notation $\mathbf{R}(\tau(\theta)) = \mathbf{R}(\tau)$ to emphasize the dependence of the cumulative reward on the parameters θ that affect the trajectory distribution.

2.2 Risk-Sensitive Reinforcement Learning

Risk-sensitivity in reinforcement learning is often associated with the following general problem:

$$\max_{\theta} \inf_{\rho_{\theta} \in \Psi} \mathbb{E}_{\tau \sim \rho_{\theta}} [\mathbf{R}(\tau(\theta))], \quad (4)$$

which induces distributional robustness with respect to the probability distribution over the possible trajectories \mathcal{T} . Maximization over the parameter space $\theta \in \mathbb{R}^d$ simulates optimization over all policies $\pi \in \Pi$. Minimization over the distributions ρ_{θ} corresponds to reducing the sensitivity of the uncertainties that affect ρ_{θ} , which include both the initial state distribution p_0 , and the transition probabilities P , i.e., all uncertainties with respect to the model parameters and any noise perturbation of the system dynamics. Typically the space Ψ is constrained to a closed set of distributions that defines a trade-off between optimality and conservativeness of the policy. However, solving (4) with dynamic programming and game theoretic methods becomes intractable in large state/action spaces, and methods that approximate its solution have been studied (Tamar et al., 2013; Delage & Mannor, 2010; Abdullah et al., 2019), including the use of different statistical measures of the objective function to avoid the minimization over the distributions ρ_{θ} (Pan et al., 2019; Dotan Di Castro & Mannor, 2012; Prashanth, 2014; Tamar, 2015; Liu et al., 2018).

In this work, we focus on the following definition of a risk-sensitive reinforcement learning problem that incorporates an inherent regularization term for the set of distributions ρ_{θ} :

$$\max_{\theta} \inf_{\hat{\rho}} -\text{sgn}(\beta) \left\{ \mathbb{E}_{\tau \sim \hat{\rho}} [\mathbf{R}(\tau)] - \frac{1}{\beta} D(\hat{\rho}, \rho_{\theta}) \right\}, \quad (5)$$

where $\text{sgn}(x) = x/|x|$ for $x \neq 0$ represents the sign operator, and $D(Q, P)$ represents the Kullback-Leibler divergence measure:

$$D(Q, P) = \begin{cases} \mathbb{E}_Q \left[\log \frac{dQ}{dP} \right] & \text{if } Q \ll P \\ \infty & \text{otherwise} \end{cases}. \quad (6)$$

The optimization problem (5) is essentially a game between the trajectory distribution $\hat{\rho}$ that tries to find a worst-case scenario of the cumulative reward while staying close to a baseline distribution ρ_θ , and the parameter vector θ that tries to optimize for the worst-case expected cumulative reward. The use of baseline terms in reinforcement learning is widely adopted (Sutton & Barto, 2018; Weaver & Tao, 2013) and is further explained in Section 3. The parameter β is the risk-sensitive parameter that controls the behavior of the agent and the weight of the regularization term. In particular, $\beta > 0$ induces a risk-seeking (optimistic) approach, while $\beta < 0$ invokes a risk-averse (pessimistic) approach. The value of β determines the trade-off between optimizing with respect to the observed reward, or with respect to staying close to the baseline trajectory distribution $\bar{\rho}_\theta$, which is a trade-off between optimality and conservativeness of the policy.

2.3 Risk-Sensitive Reinforcement Learning with Exponential Criteria

Problem (5) is still a game-theoretic formulation of the risk-sensitive reinforcement learning problem, which can be hard to solve directly. However, it is well known (see, e.g., (Föllmer & Schied, 2002; Mavridis, Noorani, & Baras, 2022; Dai Pra, Meneghini, & Runggaldier, 1996)), that the following duality relationship, with respect to a Legendre-type transform, holds:

Theorem 1. (Föllmer & Schied, 2002) Consider a measurable space (Ω, \mathcal{F}) , where \mathcal{F} is a σ -algebra on Ω . Let $\mathcal{P}(\Omega)$ be a set of probability measures $\mathbb{P} : \Omega \rightarrow [0, 1]$, and $\mathbb{P}_\mu, \mathbb{P}_\nu \in \mathcal{P}(\Omega)$. In addition, consider a bounded measurable function $Z : \Omega \rightarrow \mathbb{R}$. Then the free energy is defined as:

$$J_{l_\beta}(Z) = \frac{1}{\beta} \log \mathbb{E}_{\mathbb{P}_\mu} \left[e^{\beta Z} \right] \quad (7)$$

and the KL divergence measure:

$$D_{\text{KL}}(\mathbb{P}_\nu, \mathbb{P}_\mu) = \begin{cases} \int \log\left(\frac{d\mathbb{P}_\nu}{d\mathbb{P}_\mu}\right) d\mathbb{P}_\nu & \text{if } C_{\text{KL}}(\mathbb{P}_\nu, \mathbb{P}_\mu) \\ \infty & \text{otherwise} \end{cases} \quad (8)$$

are in duality with respect to a Legendre-type transform, in the following sense:

$$J_{l_\beta}(Z) = \begin{cases} \sup_{\mathbb{P}_\nu \in \mathcal{P}(\Omega)} \left\{ \mathbb{E}_{\mathbb{P}_\nu} [Z] - \frac{1}{\beta} D_{\text{KL}}(\mathbb{P}_\nu, \mathbb{P}_\mu) \right\}, & \beta > 0 \\ \inf_{\mathbb{P}_\nu \in \mathcal{P}(\Omega)} \left\{ \mathbb{E}_{\mathbb{P}_\nu} [Z] - \frac{1}{\beta} D_{\text{KL}}(\mathbb{P}_\nu, \mathbb{P}_\mu) \right\}, & \beta < 0 \end{cases} \quad (9)$$

Here the conditions $C_{\text{KL}}(\mathbb{P}_\nu, \mathbb{P}_\mu)$ include $\mathbb{P}_\nu \ll \mathbb{P}_\mu$ and $\int \log\left(\frac{d\mathbb{P}_\nu}{d\mathbb{P}_\mu}\right) d\mathbb{P}_\nu \in L^1(\mathbb{P}_\nu)$.

As an immediate result of Theorem 1, we get the following corollary:

Corollary 1. *The problem:*

$$\max_{\theta} J_{l_\beta}(\theta) := \frac{1}{\beta} \log \mathbb{E}_{\tau \sim \rho_\theta} \left[\exp(\beta R(\theta)) \right] \quad (10)$$

is equivalent to (5), for the baseline distribution ρ_θ being the current trajectory distribution of the algorithm, assuming that the maximum is attained.

Notice that a Taylor expansion of (10) reveals an intuition behind how the exponential criterion incorporates risk into the objective function, since it incorporates an infinite sum of the higher moments of the return, i.e., for small β we get:

$$\frac{1}{\beta} \log \mathbb{E} \left[e^{\beta R(\theta)} \right] = \mathbb{E} \left[R(\theta) \right] + \frac{\beta}{2} \text{Var} \left[R(\theta) \right] + \mathcal{O}(\beta^2) \quad (11)$$

Equation (11) shows how the risk-sensitive parameter β controls the weight of the moments of the cumulative reward in the objective function. In particular, $\beta > 0$ induces a risk-seeking (optimistic) approach, while $\beta < 0$ invokes a risk-averse approach, by subtracting the variance from the expected value of the rewards R (Noorani & Baras, 2022, 2021b). Finally, we note that as the risk-sensitive parameter β approaches zero, the exponential objective (11) approaches the risk-neutral objective (2). The sign of β in (5) fundamentally determines whether the initial optimization (with respect to ρ_θ) is a maximization or a minimization, as illustrated in equation (9). The intuitive impact of the sign of β becomes evident through the Taylor expansion in (11). Here, it is apparent that $\beta > 0$ leads to a risk-seeking (optimistic) approach, while $\beta < 0$ leads to a risk-averse (pessimistic) approach.

Remark 1. *Connection to Maximum-Entropy RL (see, e.g., (Eysenbach & Levine, 2021)). Notice that we can simplify (9) by making heuristic assumptions on the measure P_μ . In particular, it is known that the maximum-entropy objective is equivalent to the maximization of the KL-regularized objective with respect to a uniform distribution as the reference policy (Galashov et al., 2019). In other words, by assuming that P_μ is a uniform probability measure, and for $\beta > 0$, (9) and (10) yield:*

$$\max_{\theta} J_{l_\beta}(\theta) \implies \max_{\rho} \left\{ \mathbb{E}_{\tau \sim \rho} [R(\tau)] + \frac{1}{\beta} H(\rho) \right\}.$$

where $H(\rho)$ represents the Shannon entropy of the distribution ρ . Thus, we have reconstructed the maximum-entropy RL objective of (Eysenbach & Levine, 2021) as a special case of the objective (10) considered in this work.

2.4 Policy Robustness

Given an MDP $\mathcal{M}=(\mathcal{S}, \mathcal{A}, p_0, P, r, \gamma)$ with transition probabilities P , a fixed policy π , parameterized by θ , defines a trajectory distribution ρ_θ given by (1). RL algorithms try to find the optimal policy $\pi(\theta)$ given observations of the rewards r of \mathcal{M} . However, during the testing phase when the policy $\pi(\theta)$ is applied, environment and model perturbations may alter the transition probabilities. Thus, the agent is asked to operate on a perturbed MDP $\hat{\mathcal{M}}=(\mathcal{S}, \mathcal{A}, \hat{p}_0, \hat{P}, r, \gamma)$, where \hat{P} represents the perturbed system of transition probabilities. This phenomenon is especially present when training takes place in simulation environments while testing is transferred to a real system.

In this case, risk-sensitivity can be associated with a measure of robustness of a policy $\pi(\theta)$, quantified by a lower bound on the probability of good performance when the transition distribution \hat{p} during testing deviates from the distribution ρ_θ induced by $\pi(\theta)$. In this work, we will adopt the following definition of robustness of a policy $\pi(\theta)$.

Definition 1. *Let $\pi(\theta)$ be a given policy and ρ_θ be its associated trajectory distribution given by (1) with transition probabilities P . In addition, let \hat{p} be a trajectory distribution*

generated by $\pi(\theta)$ given a perturbed system of transition probabilities $\hat{\mathbb{P}}$. The policy $\pi(\theta)$ is (ξ, δ, ϵ) -robust if, for $\delta, \epsilon > 0$, and under the condition $D(\hat{\rho}, \rho_\theta) \leq \epsilon$, it holds that

$$\mathbb{P}_{\tau \sim \hat{\rho}} [\mathbf{R}(\tau(\theta)) > \xi] \geq 1 - \delta(\xi, \epsilon), \quad (12)$$

where $D(\cdot, \cdot)$ represents the KL divergence defined in (6).

In general, non-trivial sets of parameters (ξ, ϵ, δ) such that the condition (12) is satisfied cannot be found. However, for optimal policies with respect to problem (10), we can analytically provide such parameters using standard concentration inequalities. First, Theorem 2 provides upper bounds on the probability of the tails of the cumulative rewards \mathbf{R} , in the case of bounded reward, i.e., $\mathbf{R} \leq \mathbf{R}_{\max}$ almost surely. Note that $\mathbf{R}_{\max} = \frac{r_{\max}(1-\gamma^T)}{1-\gamma}$ when the per step reward is bounded $r \leq r_{\max}$.

Theorem 2. *Let $\pi(\theta^*)$ be an optimal policy with respect to (10), i.e., $\pi(\theta^*) = \operatorname{argmax}_\theta J_{l_\beta}(\theta)$, and ρ_{θ^*} be its associated trajectory distribution given by (1) with transition probabilities \mathbb{P} . In addition, let $\hat{\rho}$ be a trajectory distribution generated by $\pi(\theta)$ given a perturbed system of transition probabilities $\hat{\mathbb{P}}$ such that $D(\hat{\rho}, \rho_{\theta^*}) \leq \epsilon$. Then the following inequalities hold:*

$$\mathbb{P}_{\tau \sim \hat{\rho}} [\mathbf{R}(\tau) \leq \xi] \leq \frac{\mathbf{R}_{\max}}{\mathbf{R}_{\max} - \xi} \left(1 - \frac{1}{\mathbf{R}_{\max}} J_{l_\beta}^* + \frac{\epsilon}{|\beta| \mathbf{R}_{\max}} \right), \quad \beta < 0, \quad (13)$$

$$\mathbb{P}_{\tau \sim \hat{\rho}} [\mathbf{R}(\tau) \geq \xi] \leq \frac{1}{\xi} J_{l_\beta}^* + \frac{\epsilon}{\beta \xi}, \quad \beta > 0, \quad (14)$$

where $J_{l_\beta}^* = \frac{1}{\beta} \log \mathbb{E}_{\tau \sim \rho_{\theta^*}} \left[\exp(\beta \mathbf{R}(\tau)) \right]$.

Proof. For (14), using Markov's inequality, we get:

$$\begin{aligned} \mathbb{P}_{\tau \sim \hat{\rho}} [\mathbf{R}(\tau) \geq \xi] &\leq \frac{\mathbb{E}_{\tau \sim \hat{\rho}} [\mathbf{R}(\tau)]}{\xi} \\ &\leq \frac{1}{\xi} \left(J_{l_\beta}^* + \frac{1}{\beta} D(\hat{\rho}, \rho_{\theta^*}) \right) \\ &\leq \frac{1}{\xi} J_{l_\beta}^* + \frac{\epsilon}{\beta \xi} \end{aligned} \quad (15)$$

where we have used the duality relationship (9) for $\beta > 0$ to get:

$$\begin{aligned} J_{l_\beta}^* &= \frac{1}{\beta} \log \mathbb{E}_{\tau \sim \rho_{\theta^*}} \left[\exp(\beta \mathbf{R}(\tau)) \right] = \sup_{\rho} \left\{ \mathbb{E}_{\tau \sim \rho} [\mathbf{R}(\tau)] - \frac{1}{\beta} D(\rho, \rho_{\theta^*}) \right\} \\ &\geq \mathbb{E}_{\tau \sim \hat{\rho}} [\mathbf{R}(\tau)] - \frac{1}{\beta} D(\hat{\rho}, \rho_{\theta^*}), \end{aligned}$$

which implies that $\mathbb{E}_{\tau \sim \hat{\rho}} [\mathbf{R}(\tau)] \leq J_{l_\beta}^* + \frac{1}{\beta} D(\hat{\rho}, \rho_{\theta^*})$.

Similarly, for (13), using reverse Markov's inequality and assuming that $\mathbf{R} < \mathbf{R}_{\max}$, a.s., we get:

$$\begin{aligned} \mathbb{P}_{\tau \sim \hat{\rho}} [\mathbf{R}(\tau) \leq \xi] &\leq \frac{\mathbf{R}_{\max} - \mathbb{E}_{\tau \sim \hat{\rho}} [\mathbf{R}(\tau)]}{\mathbf{R}_{\max} - \xi} \\ &\leq \frac{\mathbf{R}_{\max}}{\mathbf{R}_{\max} - \xi} \left(1 - \frac{1}{\mathbf{R}_{\max}} J_{l_\beta}^* - \frac{1}{\mathbf{R}_{\max} \beta} D(\hat{\rho}, \rho_{\theta^*}) \right) \\ &\leq \frac{\mathbf{R}_{\max}}{\mathbf{R}_{\max} - \xi} \left(1 - \frac{1}{\mathbf{R}_{\max}} J_{l_\beta}^* + \frac{\epsilon}{|\beta| \mathbf{R}_{\max}} \right) \end{aligned} \quad (16)$$

where we have used the duality relationship (9) for $\beta < 0$ to get:

$$\begin{aligned} J_{\mathfrak{l}_\beta}^* &= \frac{1}{\beta} \log \mathbb{E}_{\tau-\rho_{\theta^*}} \left[\exp(\beta \mathbf{R}(\tau)) \right] = \inf_{\rho} \left\{ \mathbb{E}_{\tau-\rho} [\mathbf{R}(\tau)] - \frac{1}{\beta} D(\rho, \rho_{\theta^*}) \right\} \\ &\leq \mathbb{E}_{\tau-\hat{\rho}} [\mathbf{R}(\tau)] - \frac{1}{\beta} D(\hat{\rho}, \rho_{\theta^*}), \quad \beta < 0, \end{aligned}$$

which implies that $-\mathbb{E}_{\tau-\hat{\rho}} [\mathbf{R}(\tau)] \leq -J_{\mathfrak{l}_\beta}^* - \frac{1}{\beta} D(\hat{\rho}, \rho_{\theta^*})$. \square

Remark 2. Note that in Theorem 2, the term $J_{\mathfrak{l}_\beta}^* = \frac{1}{\beta} \log \mathbb{E}_{\tau-\rho_{\theta^*}} \left[\exp(\beta \mathbf{R}(\tau)) \right]$ does not depend on the perturbed system of transition probabilities $\hat{\mathbf{P}}$ in the test environment.

Equations (13) and (14) give upper bounds on the probability of the two tails of the cumulative rewards \mathbf{R} . In particular, a risk-averse agent tries to optimize for the maximum average reward weighing in the maximization of the decay of the left tail of the distribution of the total reward, while a risk-seeking agent weights in the maximization of the decay of the right tail of the reward distribution. This is consistent with the following theorem proven in (Noorani & Baras, 2022) using the Gartner-Ellis theorem of Large Deviation:

Theorem 3 ((Noorani & Baras, 2022)). *For a given negative risk parameter (risk-aversion) $\beta < 0$, the maximization of the risk-sensitive exponential criterion $J_{\mathfrak{l}_\beta}$ in (10) is equivalent to the maximization of the exponential rate of decay of the left tail of the system's trajectory reward distribution, i.e., for a given $\beta < 0$, there exists a constant $\psi \in \mathbb{R}$ such that*

$$\operatorname{argmax}_{\pi} J_{\mathfrak{l}_\beta}(\pi) = \lim_{|\tau| \rightarrow \infty} \operatorname{argmin}_{\pi} \mathbb{P}[\mathbf{R}(\tau) < \psi]$$

where $\mathbb{P}[\mathbf{R}(\tau) < \psi]$ denotes the probability of the event $\mathbf{R} < \psi$. Similarly, for a given positive risk parameter (risk-seeking) $\beta > 0$, the maximization of the risk-sensitive exponential criterion $J_{\mathfrak{l}_\beta}$ in (10) is equivalent to minimization of the exponential rate of decay of the right tail of the system's trajectory reward distribution, that is, for a given $\beta > 0$, there exists a constant ψ such that

$$\operatorname{argmax}_{\pi} J_{\mathfrak{l}_\beta}(\pi) = \lim_{|\tau| \rightarrow \infty} \operatorname{argmax}_{\pi} \mathbb{P}[\mathbf{R}(\tau) > \psi]$$

Given the results of Theorem 2, we can show that the risk-averse policy ($\beta < 0$) is a (ξ, δ, ϵ) -robust policy according to Definition 1. This is shown in Corollary 2.

Corollary 2. *Let an optimal policy $\pi(\theta^*) = \operatorname{argmax}_{\theta} J_{\mathfrak{l}_\beta}(\theta)$ with respect to (10) for $\beta < 0$. Then, $\pi(\theta^*)$ is (ξ, δ, ϵ) -robust according to Definition 1 with:*

$$\delta(\xi, \epsilon) = \frac{R_{\max}}{R_{\max} - \xi} \left(1 - \frac{1}{R_{\max}} J_{\mathfrak{l}_\beta}^* + \frac{\epsilon}{|\beta| R_{\max}} \right). \quad (17)$$

In addition, for a given $\delta = \bar{\delta}$, we can quantify ξ by:

$$\xi = R_{\max} - \frac{R_{\max}}{\bar{\delta}} \left(1 - J_{\mathfrak{l}_\beta}^* + \frac{\epsilon}{\beta R_{\max}} \right). \quad (18)$$

Proof. It follows directly from (13) since $\mathbb{P}[R > \xi] = 1 - \mathbb{P}[R \leq \xi]$. \square

So far, we have shown how the optimization problem (10) is connected to risk-sensitivity and robustness of the learned policy with respect to model perturbations. However, as will be discussed in Section 4.2, the presence of the non-linearity introduced by the logarithm in (10) creates computational problems in algorithmic implementations. For this reason, throughout the rest of this paper we will study the equivalent (in terms of optimal policy) problem:

$$\max_{\theta} J_{\beta}(\theta) := \frac{1}{\beta} \mathbb{E}_{\tau \sim \rho_{\theta}} \left[\exp(\beta R(\theta)) \right]. \quad (19)$$

The equivalence of (19) and (10), in terms of the optimal policy to be found stems from the fact that the logarithm is a strictly increasing function. Eliminating the logarithm transforms the objective function into a form that is particularly amenable to gradient-based approaches, as elucidated in greater detail in Section 4.2. The factor $1/\beta$ accounts for the sign, while simultaneously providing a scaling factor that guards against computational instability.

3. Policy Gradient Methods with Exponential Criteria

Risk-neutral policy gradient methods for reinforcement learning have been extensively studied (Tsitsiklis & Van Roy, 1997; Lewis, Vrabie, & Vamvoudakis, 2012; Gu, Lillicrap, Sutskever, & Levine, 2016). In this section, we present a brief overview of the most commonly used policy gradient RL algorithms and study their risk-sensitive counterpart based on the exponential criteria described in Section 2.3. In particular, we explore the properties of the risk-sensitive REINFORCE algorithm (Noorani & Baras, 2021a) and provide new analytic results for its implementation regarding its update rule and the convergence of its parameters.

3.1 Policy Gradient Methods

Policy Gradient (PG) methods are a class of Policy Search methods that use gradient ascend/descend schemes to search for the optimal policy (Sutton, McAllester, Singh, & Mansour, 2000; Kakade, 2001; Gu, Lillicrap, Turner, Ghahramani, Schölkopf, & Levine, 2017). The well-known REINFORCE (Williams & Peng, 1991) and Actor-Critic (Konda & Tsitsiklis, 1999) algorithms are examples of Policy Gradient algorithms, which are particularly suitable for continuous action spaces. On-policy Monte Carlo policy gradient algorithms, e.g., REINFORCE (Williams, 1992), use episode samples to estimate the gradient. That is, at each iteration of the algorithm t , the parameters of the policy are updated using the following update rule

$$\theta_{t+1} = \theta_t + \alpha \widehat{\nabla J}(\theta_t) \quad (20)$$

where $\alpha \in \mathbb{R}$ is a constant step-size, i.e., learning rate, and $\widehat{\nabla J}(\theta_t) \in \mathbb{R}^d$ is an unbiased estimate of the gradient with respect to the policy parameter θ . Monte-Carlo policy gradient estimates are unbiased estimates of the gradient of the system’s performance measure, but suffer from high variance. Such high variance estimates of the gradient lead to high sample

complexity and hinder learning. This may limit their applications, especially in real-world scenarios where collecting a large number of samples may be expensive, time-consuming, or complex.

There has been numerous variance reduction techniques for policy gradient methods to mitigate the high variance of Monte Carlo policy gradient estimates while preserving the stability and convergence properties of on-policy Monte Carlo policy gradient algorithms. These techniques attempt to reduce the variance of the gradient without introducing bias. The subtraction of an appropriately chosen baseline, both state-dependent (Williams, 1992; Sutton & Barto, 2018) and action-dependent (Thomas & Brunskill, 2017; Gu et al., 2017; Grathwohl, Choi, Wu, Roeder, & Duvenaud, 2017; Liu, Feng, Mao, Zhou, Peng, & Liu, 2017; Wu, Rajeswaran, Duan, Kumar, Bayen, Kakade, Mordatch, & Abbeel, 2018) baselines, for variance reduction in policy gradient have been studied extensively over the last two decades. The use of action-dependent baselines and their effectiveness in reducing the variance over state-dependent baselines have been the subject of much debate (Tucker, Bhupatiraju, Gu, Turner, Ghahramani, & Levine, 2018), so we refrain from considering action-dependent baselines in this work. Although an optimal state-dependent baseline exists (Weaver & Tao, 2013), it is typically hard to find.

3.2 REINFORCE: A Monte Carlo Policy Gradient Method

An estimate of the gradient of the (risk-neutral) objective of (2) with respect to the policy parameters can be obtained using the policy gradient theorem (Sutton, McAllester, Singh, & Mansour, 1999), that is,

$$\nabla J(\theta) \propto \mathbb{E}_{\tau \sim \rho_\theta} \left[R(\tau) \sum_{t=0}^{|\tau|-1} \nabla \log \pi_\theta(\mathbf{a}_t | s_t; \theta) \right] \quad (21)$$

Policy Gradient theorem suggests that the gradient estimate in Eq. (20) can be computed by Monte Carlo estimation of the expectation in Eq. (21). It is known that such estimation suffers from high variance (Sutton & Barto, 2018). To reduce variance, by taking advantage of the temporal structure of the problem and causality, it has been shown that the gradient (expected value in Eq (21)) could be re-written in terms of reward-to-go $R_t := \sum_{t'=t}^{|\tau|-1} \gamma^{t'-t} r(s_{t'}, \mathbf{a}_{t'})$ as follows:

$$\nabla J(\theta) \propto \mathbb{E}_{\tau \sim \rho_\theta} \left[\sum_{t=0}^{|\tau|-1} R_t \nabla \log \pi_\theta(\mathbf{a}_t | s_t; \theta) \right] \quad (22)$$

Using Eq. (22), the update rule in the standard REINFORCE algorithm is obtained and is given by

$$\theta_{t+1} = \theta_t + \alpha R_t \frac{\nabla \pi(\mathbf{a}_t | s_t; \theta)}{\pi(\mathbf{a}_t | s_t; \theta)}. \quad (23)$$

To enable the comparison between REINFORCE and our risk-sensitive counterpart later in Section 3.3, we summarize the REINFORCE algorithm in Algorithm 1.

Algorithm 1 REINFORCE

- 1: **Input:** a differentiable policy parametrization $\pi(\mathbf{a}|\mathbf{s};\theta)$.
 - 2: **Algorithm parameters:** step-size $\alpha>0$, discount factor $\gamma>0$, and the risk parameter β .
 - 3: **Initialization:** Initialize policy parameters $\theta \in \mathbb{R}^d$ (e.g. to 0).
 - 4: **while True do**
 - 5: **Generate an episode following the policy $\pi(\cdot|\cdot;\theta)$, i.e., $s_0\sim p_0$, $\mathbf{a}_t\sim\pi(\cdot|s_t;\theta)$ and $s_{t+1}\sim p(\cdot|s_t, \mathbf{a}_t)$, generating a sequence of state-actions $s_0, \mathbf{a}_0, \dots, s_{|\tau|-1}, \mathbf{a}_{|\tau|-1}$**
 - 6: **for $t = 0$ to $|\tau| - 1$ do**
 - 7: $\hat{R} \leftarrow \sum_{t'=t}^{|\tau|-1} \gamma^{t'-t} r_{t'}$
 - 8: $\theta_{t+1} \leftarrow \theta_t + \alpha \gamma^t \hat{R} \nabla \log \pi(\mathbf{a}_t|s_t; \theta)$
 - 9: **end for**
 - 10: **end while**
-

REINFORCE is a Monte Carlo algorithm, that is, an entire trajectory needs to be generated before an update can be computed. This limits the method to episodic settings and is prone to high variance. Such high variance hinders the learning process.

3.2.1 REINFORCE WITH BASELINE

To further reduce the variance associated with the gradient estimations of (21) and (22), which is a must in complex environments, various techniques have been employed. Baseline methods are among the most common, and are based on subtracting an appropriately chosen baseline from the reward-to-go R_t to reduce the variance without introducing bias to the estimator. Using baselines, we have (Sutton & Barto, 2018)

$$\nabla J(\theta) \propto \mathbb{E}_{\tau \sim \rho_\theta} \left[\sum_{t=0}^{|\tau|-1} \left(R_t - b(s_t) \right) \nabla \log \pi_\theta(\mathbf{a}_t|s_t; \theta) \right] \quad (24)$$

where $b(s_t)$ is a state-dependent function. State-dependent baselines are guaranteed to introduce no bias. An optimal state-dependent baseline exist, however, it is hard to find (Weaver & Tao, 2013). A common baseline in practice is the estimate of the value function, i.e., $b(s_t) = V^{\pi_\theta}(s_t)$, where

$$V^{\pi_\theta}(s_t) := \mathbb{E}_{\tau \sim \rho_\theta} \left[R_t | s_t \right]$$

Baselines have shown better convergence in practice. The effect of action-dependent baselines over state-dependent baselines is subject to debate. As we will show, a particularly convenient property of using exponential criteria is that it alleviates the need for such approaches (Noorani & Baras, 2021b). The introduction of a baseline leads to the following algorithm. Note the change in lines 8 and 9 of Algorithm 2 compared to the REINFORCE algorithm (Algorithm 1).

Algorithm 2 REINFORCE with Baseline (value function approximation as baseline)

- 1: **Input:** a differentiable policy parametrization $\pi(\mathbf{a}|s; \theta)$.
 - 2: **Algorithm parameters:** step-sizes $\alpha > 0$ and $\bar{\alpha} > 0$, discount factor $\gamma > 0$, and the risk parameter β .
 - 3: **Initialization:** Initialize policy parameters $\theta \in \mathbb{R}^d$ (e.g. to 0) and value parameters $w \in \mathbb{R}^{d'}$.
 - 4: **while True do**
 - 5: **Generate an episode following the policy $\pi(\cdot|\cdot; \theta)$, i.e., $s_0 \sim p_0$, $\mathbf{a}_t \sim \pi(\cdot|s_t; \theta)$ and $s_{t+1} \sim p(\cdot|s_t, \mathbf{a}_t)$, generating a sequence of state-actions $s_0, \mathbf{a}_0, \dots, s_{|\tau|-1}, \mathbf{a}_{|\tau|-1}$**
 - 6: **for $t = 0$ to $|\tau| - 1$ do**
 - 7: $\hat{R} \leftarrow \sum_{t'=t}^{|\tau|-1} \gamma^{t'-t} r_{t'}$
 - 8: $\theta_{t+1} \leftarrow \theta_t + \alpha \gamma^t (\hat{R} - V(s_t; w_t)) \nabla \log \pi(\mathbf{a}_t | s_t; \theta)$
 - 9: $w_t = w_t + \bar{\alpha} \gamma^t (\hat{R} - V(s_t; w_t)) \nabla V(s_t; w_t)$
 - 10: **end for**
 - 11: **end while**
-

3.3 Risk-sensitive REINFORCE (R-REINFORCE)

Risk-sensitive REINFORCE (R-REINFORCE) (Noorani & Baras, 2021a) is a Monte Carlo algorithm, similar to REINFORCE (Williams & Peng, 1991), that seeks to find the optimal policy for the proposed risk-sensitive exponential criteria. In R-REINFORCE, the update rule is given by:

$$\nabla J_{\theta}(\theta) \propto \frac{1}{\beta} \mathbb{E}_{\tau \sim \rho_{\theta}} \left[\sum_{t=0}^{|\tau|-1} e^{\beta R_t} \nabla \log \pi_t(\theta) \right] \quad (25)$$

where $R_t := \sum_{t'=t}^{|\tau|-1} \gamma^{t'-t} r(s_{t'}, \mathbf{a}_{t'})$. The derivation of this formula is based on a risk-sensitive variation of the policy gradient theorem (Sutton et al., 1999). These results are provided in Appendix A. Given (25), the R-REINFORCE update rule reads as:

$$\theta_{t+1} = \theta_t + \frac{\alpha}{\beta} e^{\beta R_t} \frac{\nabla \pi(\mathbf{a}_t | s_t; \theta)}{\pi(\mathbf{a}_t | s_t; \theta)}. \quad (26)$$

and is a stochastic approximation algorithm (see, e.g., (Borkar, 2009)). We provide the convergence analysis of the parameters θ in Appendix A.1. The implementation of the Risk-sensitive REINFORCE algorithm is given in Alg. 3 where the differences with the (risk-neutral) REINFORCE algorithm (Alg. 1) are highlighted. For more details, the readers are referred to (Noorani & Baras, 2021a) and the references therein.

Algorithm 3 Risk-sensitive REINFORCE

- 1: **Input:** a differentiable policy parametrization $\pi(\mathbf{a}|\mathbf{s};\theta)$.
 - 2: **Algorithm parameters:**
step-size $\alpha>0$, discount factor $\gamma>0$, and the risk parameter β .
 - 3: **Initialization:** Initialize policy parameters $\theta \in \mathbb{R}^d$ (e.g. to 0).
 - 4: **while True do**
 - 5: **Generate an episode following the policy** $\pi(\cdot|\cdot;\theta)$,
i.e., $s_0 \sim p_0$, $\mathbf{a}_t \sim \pi(\cdot|s_t;\theta)$ and $s_{t+1} \sim p(\cdot|s_t, \mathbf{a}_t)$,
generating a sequence of state-actions $s_0, \mathbf{a}_0, \dots, s_{|\tau|-1}, \mathbf{a}_{|\tau|-1}$
 - 6: **for** $t = 0$ **to** $|\tau| - 1$ **do**
 - 7: $\hat{R} \leftarrow \sum_{t'=t}^{|\tau|-1} \gamma^{t'-t} r_{t'}$
 - 8: $\theta_{t+1} \leftarrow \theta_t + \alpha \gamma^t \frac{1}{\beta} e^{\beta \hat{R}} \nabla \log \pi(\mathbf{a}_t|s_t; \theta_t)$
 - 9: **end for**
 - 10: **end while**
-

Note that the update rule is not proportional to the reward-to-go $R_t := \sum_{t'=t}^{|\tau|-1} \gamma^{t'-t} r(s_{t'}, \mathbf{a}_{t'})$, but to the exponential d

$$\beta e^{\beta R_t} = \frac{1}{\beta} \prod_{t'=t}^{|\tau|-1} \exp\{\gamma^{t'-t} \beta r(s_{t'}, \mathbf{a}_{t'})\} \tag{27}$$

This is a significant difference since it yields to the multiplicative risk-sensitive Bellman’s equation discussed in Section 4.2. In addition, notice that for the case of always positive (resp. negative) reward and negative (resp. positive) risk parameter β , a very high (resp. low) reward gets exponentially small (resp. large) weight resulting in a risk-averse behavior.

Remark 3. *By substituting the exponential with its Taylor series expansion (see eq. (11)), we can see that the risk-sensitive objective provides a natural baseline (see Section 3.2.1). This is empirically shown in (Noorani & Baras, 2021a). The baseline term can be derived by expanding the exponential function and combining all terms, except for the one proportional to R_t , i.e., $\nabla J(\theta) \propto \mathbb{E}_{\tau \sim \rho_\theta} \left[\sum_{t=0}^{|\tau|-1} (R_t - b(s_t)) \nabla \log \pi_\theta(\mathbf{a}_t|s_t; \theta) \right]$ where $b(s_t) = -(\frac{1}{\beta} + \frac{\beta R_t^2}{2} + \dots)$. In Section 5, we show that such baseline leads to significant variance reduction and acceleration of learning process.*

4. Actor-Critic Methods with Exponential Criteria

Recall that REINFORCE algorithms of Alg. 1 (without baseline) and Alg. 2 (with baseline) are Monte Carlo algorithms and limited to episodic settings. To enable online update and extend to non-episodic settings, Actor-Critic algorithms (Konda & Tsitsiklis, 1999; La & Ghavamzadeh, 2013) improve the policy using gradient methods and use a critic network to estimate the value function and use it to bootstrap an estimate of the reward-to-go. That is, the estimate of the reward-to-go $R_t := \sum_{t'=t}^{|\tau|-1} \gamma^{t'-t} r(s_{t'}, \mathbf{a}_{t'})$ is computed using the estimated/learned value function. Bootstrapping enables Actor-Critic methods to use an online update rule; eliminating the need to generate the entire trajectory before making an update and learning. This further extends the method to non-episodic settings

and reduces the variance. Furthermore, Actor-critic methods (Konda & Tsitsiklis, 2003; La & Ghavamzadeh, 2013; Bhatnagar, Sutton, Ghavamzadeh, & Lee, 2009) attempt to reduce the variance with replacing the Monte Carlo estimate with an estimate based on the sampled return and a function approximator. In particular, the ‘actor’ implements a policy gradient algorithm based on a function approximation estimated and updated by the ‘critic’ with every observation. Actor-critic methods have lower variance but introduce bias from the function approximation. This bias leads to instability and high sensitivity to hyperparameters. Actor-critic methods have been studied for mean-variance in (La & Ghavamzadeh, 2013). Function approximation can be used to estimate R_t by the value function $V^{\pi_\theta}(s_t) \simeq \mathbb{E}_{\tau \sim \rho_\theta}[R_t | s_t]$, which can be shown to satisfy the Bellman’s equation

$$V^{\pi_{\theta^*}}(s) = \mathbb{E}_{\mathbf{a} \sim \pi_{\theta^*}} \left[r(s, \mathbf{a}) + \gamma V^{\pi_{\theta^*}}(s') | s \right] \quad (28)$$

where we use $\pi_\theta := \pi(\mathbf{a} | s; \theta)$ as a shorthand notation. The fact that (28) is a contraction mapping has given rise to stochastic approximation algorithms that try to asymptotically minimize the mean-squared error

$$\min_{\theta} \mathbb{E}_{\mathbf{a} \sim \pi_\theta} \left[\| r(s, \mathbf{a}) + \gamma V^{\pi_\theta}(s') - V^{\pi_\theta}(s) \|^2 | s \right]$$

a fact that is used by Temporal-Difference RL methods that employ learning models (e.g. neural networks (Gu et al., 2016) or other learning algorithms (Mavridis & Baras, 2021; Mavridis, Suriyarachchi, & Baras, 2021)) to learn the optimal function $V^{\pi_{\theta^*}}$.

4.1 Online Actor-Critic Algorithms

Online RL methods are mainly represented by Actor-Critic (AC) methods that use two learning systems (e.g., neural networks) to estimate the parameters θ_t of the optimal policy $\pi(\mathbf{a}_t | s_t; \theta_t)$ (actor) and the parameters w_t of the value function $V(s_t; w_t)$ (critic), that is

$$\begin{cases} \theta_{t+1} = \theta_t + \alpha \left(\hat{R}_t - V(s_t; w_t) \right) \frac{\nabla \pi(\mathbf{a}_t | s_t; \theta_t)}{\pi(\mathbf{a}_t | s_t; \theta_t)} \\ w_{t+1} = w_t - \bar{\alpha} \nabla J_c(s_t; w_t, \theta_t) \end{cases} \quad (29)$$

where $J_c(s_t; w_t, \theta_t) = \|\hat{R}_t - V(s; w_t)\|^2$. In this case, \hat{R}_t is given by

$$\hat{R}_t := r(s, \pi_{\theta_t}) + \gamma V(s'; w_t)$$

where \hat{R}_t is an estimate of the reward-to-go R_t , and the form of the objective function J_c of the critic is what gives it the name Temporal-Difference (TD) learning. The algorithmic implementation is provided in Alg. 4. Special consideration needs to be given to the stepsizes $\{\alpha, \bar{\alpha}\}$ as their choice heavily affects the learning process. The stepsizes $\{\alpha, \bar{\alpha}\}$ should decrease with time according to the theory of stochastic approximation algorithms (Borkar, 2009; Mavridis & Baras, 2022), i.e., $\sum_n \alpha(n) = \infty$, and $\sum_n \alpha^2(n) < \infty$, a fact that is often overlooked in practice. In addition, according to the theory of two-timescale stochastic approximation algorithms, the actor recursions should run at a higher time-scale, which is satisfied by the condition $\bar{\alpha}/\alpha \rightarrow 0$ (Borkar, 2009).

Algorithm 4 Online Actor-Critic

- 1: **Input:** a differentiable policy parametrization $\pi(\mathbf{a}|\mathbf{s};\theta)$.
 - 2: **Algorithm parameters:** step-sizes $\alpha>0$ and $\bar{\alpha}>0$, discount factor $\gamma>0$, and the risk parameter β .
 - 3: **Initialization:** Initialize policy parameters $\theta \in \mathbb{R}^d$ and value parameters $w \in \mathbb{R}^{d'}$ (e.g. to 0) (e.g. to 0).
 - 4: **while True do**
 - 5: **for** $t = 0$ **to** $|\tau| - 1$ **do**
 - 6: **Starting at an initial state** s_0 , **take an action by following the current policy** $\mathbf{a}_t \sim \pi(\cdot|s_t; \theta)$ **and observe the successor state** $s_{t+1} \sim p(\cdot|s_t, \mathbf{a}_t)$, **and the reward** r_t
 - 7: $\hat{R} \leftarrow r_t + \gamma V(s_{t+1}, w_t)$
 - 8: $\theta_{t+1} \leftarrow \theta_t + \alpha \gamma^t (\hat{R} - V(s_t; w_t)) \nabla \log \pi(\mathbf{a}_t | s_t; \theta)$
 - 9: $w_{t+1} = w_t + \bar{\alpha} \gamma^t (\hat{R} - V(s_t; w_t)) \nabla V(s_t; w_t)$
 - 10: **end for**
 - 11: **end while**
-

4.2 Risk-Sensitive Bellman Equation

To introduce online updates that are not based on Monte Carlo simulation, we need to study the risk-sensitive counterparts of the Bellman equation. Recall that, in risk-neutral Reinforcement Learning, we are solving the optimal control problem

$$\max_{\pi} \mathbb{E} \left[\sum_{l=0}^{\infty} \gamma^l r(s_l, \mathbf{a}_l) \right], \quad \mathbf{a}_l \sim \pi(\cdot|s_l) \quad (30)$$

where the expectation is computed over the space of the states s_l (based on the transition probabilities) while the actions are given by $\mathbf{a}_l \sim \pi(\cdot|s_l)$. This gives rise to the definition of the value function V^π of a policy π as $V^\pi(s_k) := \mathbb{E} \left[\sum_{l=k}^{\infty} \gamma^{l-k} r(s_l, \mathbf{a}_l) | s_k \right]$. As a result of Bellman's principle, we get the (discrete-time) Hamilton-Jacobi-Bellman (HJB) equation

$$V^*(s_k) := \max_{\pi} \mathbb{E} \left[\sum_{l=k}^{\infty} \gamma^{l-k} r(s_l, \mathbf{a}_l) | s_k \right] = \max_{\pi} \{ r(s_k, \mathbf{a}_k) + \gamma \mathbb{E} [V^*(s_{k+1}) | s_k] \} \quad (31)$$

In contrast to the risk-neutral case, in the risk-sensitive reinforcement learning setting the optimal control problem is often associated with an undiscounted version of the cost function \bar{J}_{l_β} in (10) and reads as:

$$\max_{\pi} \bar{J}_{l_\beta}(\pi) := \limsup_n \frac{1}{n} \log \mathbb{E} \left[e^{\beta \sum_{l=0}^{n-1} r(s_l, \mathbf{a}_l)} | s_0 \right], \quad \mathbf{a}_l \sim \pi(\cdot|s_l) \quad (32)$$

Notice that it has been assumed that $\gamma = 1$, and the average limit has been added to ensure boundedness of the cost. It has been shown (see, e.g., (Borkar, 2002, 2010)) that by defining a value function $\bar{V}_{l_\beta}^*(s_k) = \max_{\pi} \mathbb{E} \left[e^{\beta \sum_{l=k}^{t_h} r(s_l, \mathbf{a}_l) - \log J_{l_\beta}^*} | s_k \right]$, $\mathbf{a}_l \sim \pi(\cdot|s_l)$, with t_h being the

first hitting time of a distinguished state, problem (32) is equivalent to a multiplicative version of the Bellman equation which defines a nonlinear eigenvalue problem:

$$\bar{V}_{l_\beta}^*(s_k) = \max_{\pi} \frac{e^{\beta r(s_k, a_k)}}{J_{l_\beta}^*} \mathbb{E} \left[V_{l_\beta}^*(s_{k+1}) | s_k \right], \quad a_k \sim \pi(\cdot | s_k) \quad (33)$$

For sufficiently small β , stochastic approximation updates in two timescales can be designed to solve the eigenvalue problem recursively implementing a policy iteration scheme and converging to an optimal stationary control that attains the optimal reward $J_{l_\beta}^* < \infty$. It is important to point out that substituting for the logarithmic value function $W(\cdot) = \log V_{l_\beta}(\cdot)$ results in an additive dynamic programming equation, that has similarities with the classical equation for average reward:

$$W^*(s_k) := \max_{\pi} \left\{ r(s_k, a_k) + \log \mathbb{E} \left[e^{W^*(s_{k+1})} | s_k \right] \right\} - \log J_{l_\beta}^* \quad (34)$$

While this seems like a compelling formulation, and has indeed been followed by some authors (see, e.g., (Fei et al., 2020; Fei, Yang, Chen, & Wang, 2021)), the problem arises when attempting to formulate a reinforcement learning algorithm out of the latter dynamic programming equation. In particular, notice that, in eq. (34), the conditional expectation with respect to the transition probabilities appears inside a logarithm, in contrast to eq. (38). This typically leads to a violation of the assumptions of the stochastic approximation algorithm used to train temporal-difference RL algorithms (e.g., stochastic gradient descent if using neural networks) (Borkar, 2010). As a result, the form of eq. (34) is not convenient for Q-learning and most temporal-difference RL methods.

In this work, we consider the discounted optimal control problem:

$$\max_{\pi} J_{\beta}(\pi) := \frac{1}{\beta} \mathbb{E} \left[e^{\beta \sum_{l=0}^{\infty} \gamma^l r(s_l, a_l)} \right], \quad a_l \sim \pi(\cdot | s_l) \quad (35)$$

as introduced in (19). According to the cost function J_{β} , we define the risk-sensitive value function of a policy π as

$$V_{\beta}^{\pi}(s_k) := \frac{1}{\beta} \mathbb{E} \left[e^{\beta \sum_{l=k}^{\infty} \gamma^{l-k} r(s_l, a_l)} | s_k \right], \quad a_l \sim \pi(\cdot | s_l) \quad (36)$$

We further define:

$$\bar{V}_{\beta}^{\pi}(s_k) := \beta V_{\beta}^{\pi}(s_k) = \mathbb{E} \left[e^{\beta \sum_{l=k}^{\infty} \gamma^{l-k} r(s_l, a_l)} | s_k \right], \quad a_l \sim \pi(\cdot | s_l) \quad (37)$$

By definition, we get that $\bar{V}_{\beta}^{\pi}(\cdot) \geq 0$, and the following relationship holds for $\gamma \approx 1$:

$$\begin{aligned} \bar{V}_{\beta}^*(s_k) &:= \max_{\pi} \mathbb{E} \left[e^{\beta \sum_{l=k}^{\infty} \gamma^{l-k} r(s_l, a_l)} | s_k \right] \\ &= \max_{\pi} \mathbb{E} \left[e^{\beta(r(s_k, a_k) + \gamma \sum_{l=k+1}^{\infty} \gamma^{l-(k+1)} r(s_l, a_l))} | s_k \right] \\ &\approx \max_{\pi} e^{\beta r(s_k, a_k)} \mathbb{E} \left[(\bar{V}_{\beta}^*)^{\gamma}(s_{k+1}) | s_k \right] \\ &= \max_{\pi} \mathbb{E} \left[e^{\beta r(s_k, a_k) + \gamma \log \bar{V}_{\beta}^*(s_{k+1})} | s_k \right] \end{aligned} \quad (38)$$

where $\bar{V}^*(\cdot) = \bar{V}^{\pi^*}(\cdot)$ is the optimal value function resulting by the optimal control policy. Note that equality in (38) holds in the case of $\gamma = 1$, which is the known nonlinear eigenvalue problem (Borkar, 2010). To see that, one makes use of the law of total expectation to get $\mathbb{E} \left[e^{\beta \sum_{i=k+1}^{\infty} r(s_i, a_i)} | s_k \right] = \mathbb{E} \left[\mathbb{E} \left[e^{\beta \sum_{i=k+1}^{\infty} r(s_i, a_i)} | s_{k+1} \right] | s_k \right] = \mathbb{E} \left[(\bar{V}_\beta^*)(s_{k+1}) | s_k \right]$.

Notice how the use of the exponential has resulted in a multiplicative version of the Bellman equation as well. In Section 4.3, we will make use of this relationship to design an actor-critic approach based on the stochastic approximation updates of eq. (26), where a critic model will be used to recursively estimate the value function given in (38).

4.3 Risk-Sensitive Online Actor-Critic (R-AC)

To develop a risk-sensitive temporal-difference reinforcement learning algorithm, we use two learning systems (e.g., neural networks) to estimate the optimal policy (actor) and risk-sensitive value function (critic), similar to Section 4.1. That is, we keep two learning algorithms as follows:

$$\begin{cases} \theta_{t+1} = \theta_t + \alpha \frac{1}{|\beta|} (R_t^\beta - \bar{V}_\beta(s_t; \mathbf{w}_t)) \frac{\nabla \pi(\mathbf{a}_t | s_t; \theta_t)}{\pi(\mathbf{a}_t | s_t; \theta_t)} \\ \mathbf{w}_{t+1} = \mathbf{w}_t - \bar{\alpha} \nabla J_r(s_t; \mathbf{w}_t, \theta_t) \end{cases} \quad (39)$$

where, in contrast to the risk-neutral case, here $R_t^\beta = \exp[\beta r(s_t, \mathbf{a}_t) + \gamma \log \bar{V}_\beta(s_{t+1}; \mathbf{w}_t)]$ and J_r is defined as:

$$J_r(s_t; \mathbf{w}_t, \theta_t) = \|\exp[\beta r(s_t, \mathbf{a}_t) + \gamma \log \bar{V}_\beta(s_{t+1}; \mathbf{w}_t)] - \bar{V}_\beta(s_t; \mathbf{w}_t)\|^2, \quad \mathbf{a} \sim \pi_{\theta_t} \quad (40)$$

which is a stochastic gradient descent approach to asymptotically minimize the mean-squared error:

$$\min_{\mathbf{w}} \mathbb{E} \left[\|e^{\beta r(s_t, \mathbf{a}_t)} (\bar{V}_\beta)^\gamma(s_{t+1}; \mathbf{w}) - \bar{V}_\beta(s_t; \mathbf{w})\|^2 | s_t \right], \quad \mathbf{a} \sim \pi_{\theta_t}$$

The actor parameter updates constitute a stochastic approximation algorithm based on (26), where the average reward-to-go $V_\beta(s_t; \mathbf{w}_t) = \frac{1}{\beta} \mathbb{E} [e^{\beta R_k} | s_k]$ is estimated by the critic model. The critic parameter updates are again a stochastic approximation scheme that should run in a lower timescale (see Section 4.1) and estimate the optimal weights of the value function by minimizing the error: Notice that this recursion does not correspond to a fixed-point iteration but rather to a stochastic gradient descent approach.

Remark 4. Note that simply minimizing the error $\| \beta e^{\beta r(s, \mathbf{a})} + \gamma V(s'; \mathbf{w}_t) - V(s; \mathbf{w}_t) \|$, $\mathbf{a} \sim \pi_{\theta_t}$, for the value function V defined in (31) is not equivalent to the above update rule, but it is rather equivalent to scaling the initial rewards r_t to $\beta e^{\beta r_t}$. This would result in the substitution of the product term with a summation in Eq. (27), and is a fundamentally different performance criterion.

Remark 5. The exponent γ is constrained to be a rational number such that the term V_β^γ is well-defined. However, it is not a good practice to compute the term V_β^γ directly as it requires the application of a power operation with the non-integer exponent γ . For this reason, the term $\exp(\gamma \log V_\beta) = V_\beta^\gamma$ is used in the updates of Alg. 5, leading to a similar update law to the risk-neutral case.

The algorithmic implementation is based on the updates in (39) and the objective function in (40) and is provided in Alg. 5. Additional comments regarding the implementation and computational difficulties of this approach are given in Remark 5. The remarks on the stepsizes $\{\alpha, \bar{\alpha}\}$ regarding the two-timescale approach hold similarly to Section 4.1, i.e., the iterations for the actor run in a higher timescale than these of the critic model.

Algorithm 5 Risk-sensitive Online Actor-Critic (R-AC)

- 1: **Input:** a differentiable policy parametrization $\pi(\mathbf{a}|\mathbf{s};\theta)$.
 - 2: **Algorithm parameters:**
step-sizes $\alpha>0$ and $\bar{\alpha}>0$, discount factor $\gamma>0$, and the risk parameter β .
 - 3: **Initialization:** Initialize policy parameters $\theta \in \mathbb{R}^d$
and value parameters $w \in \mathbb{R}^{d'}$ (e.g. to 0).
 - 4: **while True do**
 - 5: **for** $t = 0$ **to** $|\tau| - 1$ **do**
 - 6: **Starting at an initial state** s_0 ,
 take an action by following the current policy $\mathbf{a}_t \sim \pi(\cdot|s_t; \theta)$
 and observe the successor state $s_{t+1} \sim p(\cdot|s_t, \mathbf{a}_t)$, **and the reward** r_t
 - 7: $\hat{R}_\beta \leftarrow \beta r_t + \gamma \log \bar{V}_\beta(s_{t+1}; w_t)$
 - 8: $\theta_{t+1} \leftarrow \theta_t + \alpha \gamma^t \frac{1}{|\beta|} (e^{\hat{R}_\beta} - \bar{V}_\beta(s_t; w_t)) \nabla \log \pi(\mathbf{a}_t|s_t; \theta)$
 - 9: $w_{t+1} \leftarrow w_t + \bar{\alpha} \gamma^t (e^{\hat{R}_\beta} - \bar{V}_\beta(s_t; w_t)) \nabla \bar{V}_\beta(s_t; w_t)$
 - 10: **end for**
 - 11: **end while**
-

5. Experiments

To evaluate the effectiveness of the proposed risk-sensitive reinforcement learning algorithms, we compare them against their risk-neutral counterparts on two classic reinforcement learning problems, namely the inverted pendulum (Cart-Pole) (Barto, Sutton, & Anderson, 1983) and the underactuated double pendulum (Acrobot) (Sutton, 1995).

The experiments are designed to investigate the performance and robustness of the proposed risk-sensitive algorithms against model perturbations. We quantify the performance of the algorithms using the mean values of the the observed cumulative rewards R during testing in different environments, and their robustness using the variance and the Conditional Value at Risk (CVaR) values, defined by¹:

$$\text{CVaR}_p(R) = \mathbb{E}[R | R \leq \text{VaR}_p(R)], \quad (41)$$

where p denotes the confidence interval and the Value at Risk $\text{VaR}_p(R)$ is the p -quantile of the trajectory reward given by:

$$\text{VaR}_p(R) = \inf\{r \in \mathbb{R} : P(R \leq r) > p\},$$

In particular, we make use of two p -quantiles for $p \in \{0.1, 0.9\}$ to capture the two tails of the distribution of R (see discussion in Section 5.1).

1. Definition (41) captures the intuition behind the statistical meaning of CVaR and holds if there is no probability atom at $\text{VaR}_p(R)$. For a more general definition the readers are referred to (Chow & Ghavamzadeh, 2014) and the references therein.

5.1 On the sign and values of the parameter β

The sign of the risk parameter β determines the optimization problem that is being solved according to (5). In particular, $\beta > 0$ induces a risk-seeking (optimistic) approach, while $\beta < 0$ invokes a risk-averse approach. As shown in Section 2.4, the sign of the parameter β determines which tail of the distribution of the total reward that is being weighted in the optimization process. This is consistent with our intuition that a risk-averse agent tries to optimize for the maximum average reward by weighing in the maximization of the decay of the left tail of the distribution of the total reward, while a risk-seeking agent weights in the maximization of the decay of the right tail of the reward distribution.

Thus, in the simulated experiments of Sections 5.2 and 5.3, it is expected that the risk-averse approach ($\beta < 0$) reduces the variance (and CVaR_p values for $p > 0.5$) of the distribution of the total reward. In addition, the risk-seeking approach ($\beta > 0$) does not guarantee, but can also help reduce the variance (and CVaR_p values for $p < 0.5$) of the distribution of the total reward. Such a reduction can be indicative of a better suited learning behavior for the RL policies estimated by the proposed algorithm compared to the risk-neutral RL methods. Since in the risk-seeking (or “optimistic”) case of $\beta > 0$, emphasis is given on the right tail of the distribution of the total reward, convergence to policies with high average return can be accelerated under certain values of the hyper-parameters of the system and certain sequences of random exploratory actions. The hyper-parameters that can affect this behavior include, for example, the learning rate of the actor and critic models, and random sequences that generate the exploratory actions. The selection of the policies that yield the best performance among different runs (e.g. runs with different learning rates) is often adopted. In this case, the risk-seeking approach can also lead to better policies in terms of reduced variance.

We note that in the experiments of Sections 5.2 and 5.3, we do not optimize for the risk-sensitive hyper-parameter β . Rather, we include a comparison and a sensitivity analysis for different values of β close to zero. As the risk-sensitive parameter β approaches zero, the optimization of the exponential criteria approaches the risk-neutral objective. We have included an experimental study of the risk parameter and its impact on the learning process in the proceeding sections. Further analysis and experimentation regarding the sensitivity of the optimization iterations with respect to the values of $\beta \in (0, \infty)$ is beyond the scope of this paper.

5.2 Inverted Pendulum (Cart-Pole)

The Cart-Pole problem is the classical inverted pendulum control problem, in which the agent is tasked to balance a pole mounted on a moving cart by an un-actuated joint (Barto et al., 1983). The state variable of the cart-pole system has four components $(x, \theta, \dot{x}, \dot{\theta})$, where x and \dot{x} are the position and velocity of the cart on the track, and θ and $\dot{\theta}$ are the angle and angular velocity of the pole with the vertical. The action space consists of an impulsive “left” or “right” force $F \in \{-10, +10\}N$ of fixed magnitude to the cart at discrete time intervals. A reward of $r_t = +1$ is given for each time-step t that the pole kept balanced. An episode terminates successfully after $N_t = 200$ timesteps, and the average number of timesteps $\hat{N}_t \leq N_t$ (as well as its variance) across different attempts, is used to quantify the performance of the learning algorithm. Failure occurs when $|\theta| > 12^\circ$ or when $|x| > 2.4m$.

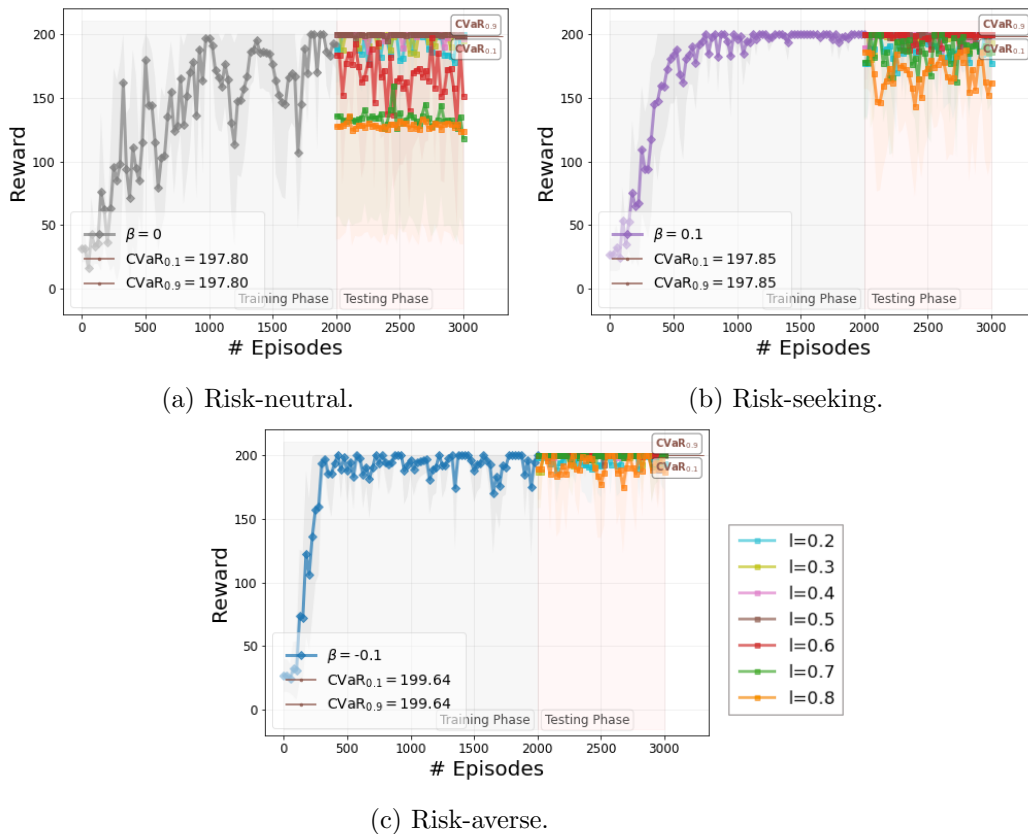


Figure 2: Training and testing behavior of the risk-neutral REINFORCE (Alg. 1) algorithm against the proposed risk-sensitive R-REINFORCE algorithm (Alg. 3) for $\beta = -0.1$ and $\beta = +0.1$ in the Cart-Pole problem. Average reward, $\text{CVaR}_{0.1}$, and $\text{CVaR}_{0.9}$ values (for $l = 0.5$) are computed over 10 independent training and testing runs with different random seeds.

In Figure 2 we present the training and testing behavior of the risk-neutral REINFORCE (Alg. 1) algorithm against the proposed risk-sensitive R-REINFORCE algorithm (Alg. 3) for $\beta = -0.1$ and $\beta = +0.1$ in the Cart-Pole problem.

We note that the use of REINFORCE with baseline (Alg. 2) yielded no statistically significant results compared to risk-neutral REINFORCE (Alg. 1). The policy networks of the algorithms are modeled as fully connected artificial neural networks with one hidden layer of only $h = 16$ neurons and a ‘ReLU’ activation function. The objective functions to be optimized are as defined in Section 3. We use a discount factor of $\gamma = 0.99$ and the ‘Adam’ optimizer. The best-performing learning rate within the set $\{0.001, 0.003, 0.005, 0.007, 0.01\}$ across all algorithms are selected for the visual inspection of the learning curves. The algorithms are trained for $n_e = 2000$ episodes in a training environment where the pole length is $l = 0.5$ and tested in different testing environments for $n_e = 1000$ testing runs where the length of the pole is perturbed such that $l \in [0.2, 0.8]$. The average reward for the different testing environments, as well as the $\text{CVaR}_{0.1}$, and $\text{CVaR}_{0.9}$ values for the testing

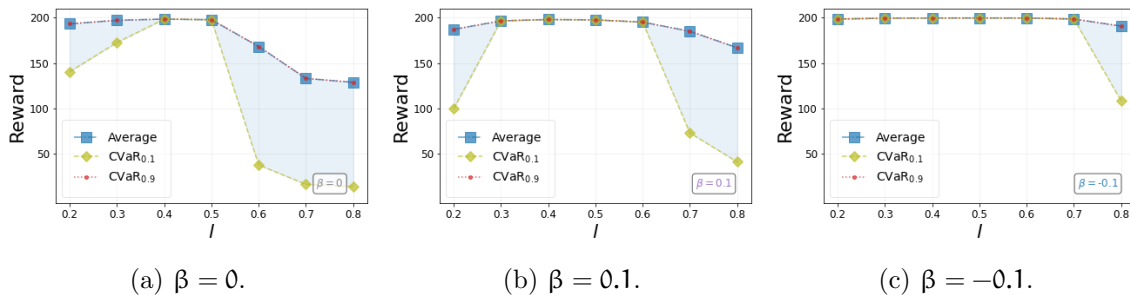


Figure 3: Robustness of risk-neutral REINFORCE (Alg. 1) and risk-sensitive R-REINFORCE (Alg. 3) algorithms in a cart-pole environment with respect to varying pole lengths. The training environment is modeled with pole length $l = 0.5$. The testing environments have perturbed pole length values of $l \in [0.2, 0.8]$. Average reward, CVaR_{0.1}, and CVaR_{0.9} values are computed over 10 independent training and testing runs with different random seeds.

environment without perturbations ($l = 0.5$) are computed over 10 independent training and testing runs with different random seeds.

We notice that although the mean, CVaR_{0.1}, and CVaR_{0.9} metrics are not significantly different across the three algorithms, the risk-sensitive algorithms in Fig. 2c and Fig. 2b converge faster to a near-optimal policy that shows increased robustness with respect to model perturbations. This is further assessed in Fig. 3, where the robustness of the algorithms with respect to model perturbations is quantified by the CVaR_{0.1}, and CVaR_{0.9} values for all testing environments. In Fig. 3a, we observe that the risk-neutral REINFORCE algorithm is performing very well near $l = 0.5$, i.e., where no model perturbations exist, but the performance is quickly deteriorated (CVaR_{0.1} values decrease) in the presence of perturbations. Fig. 3b and Fig. 3c show that the risk-sensitive approaches increase the domain of perturbations where the behavior of the RL agent is stable, with the risk-averse approach ($\beta < 0$) showcasing the best behavior.

In Figure 4 we present the training and testing behavior of the risk-neutral Online Actor-Critic (OAC) (Alg. 4) and risk-sensitive actor critic (R-AC) (Alg. 5) algorithms in the cart-pole environment with respect to varying pole length. The policy networks of the algorithms are modeled as fully connected artificial neural networks with one hidden layer of only $h = 16$ neurons and a ‘ReLU’ activation function. The objective functions to be optimized are as defined in Section 4.1. We use a discount factor of $\gamma = 0.99$ and the ‘Adam’ optimizer with the best-performing learning rates within the set $\{0.0003, 0.0005, 0.0007, 0.001\}$ across all algorithms. The best-performing learning rate are chosen best on visual inspection of the learning curves. The algorithms are trained for $n_e = 2000$ episodes in a training environment where the pole length is $l = 0.5$ and tested in different testing environments for $n_e = 1000$ testing runs where the length of the pole is perturbed such that $l \in [0.2, 0.8]$. The average reward for the different testing environments, as well as the CVaR_{0.1}, and CVaR_{0.9} values for the testing environment without perturbations ($l = 0.5$) are computed over 10 independent training and testing runs with different random seeds.

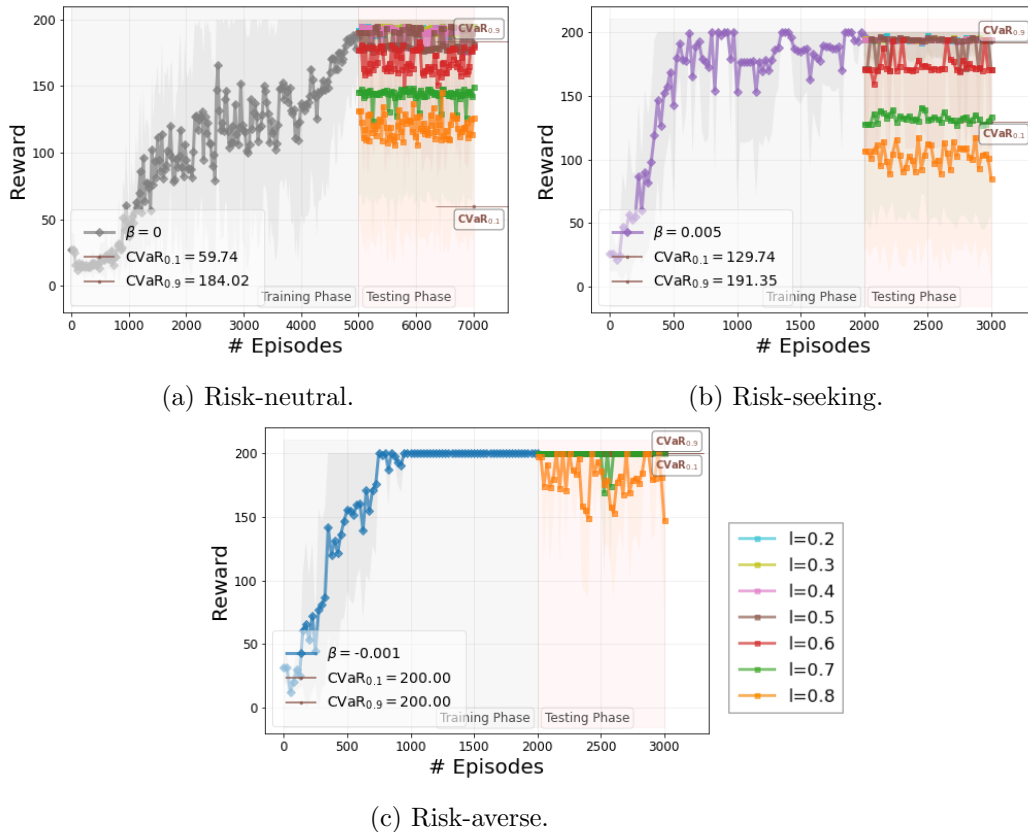


Figure 4: Training and testing behavior of the risk-neutral Online Actor-Critic (OAC) (Alg. 4) algorithm against the proposed risk-sensitive R-AC algorithm (Alg. 5) for $\beta = -0.001$ and $\beta = +0.005$ in the Cart-Pole problem. Average reward, $\text{CVaR}_{0.1}$, and $\text{CVaR}_{0.9}$ values (for $l = 0.5$) are computed over 10 independent training and testing runs with different random seeds.

We notice that although the mean value performance is not significantly different across the three algorithms, the risk-sensitive algorithms in Fig. 4c and Fig. 4b converge to a near-optimal policy (in the risk-averse case the performance is optimal) that shows reduced variation across different runs, as indicated by the $\text{CVaR}_{0.1}$, and $\text{CVaR}_{0.9}$ values calculated for $l = 0.5$ (no model perturbations). Moreover, notice that the risk-neutral algorithm in 4a is trained for $n_e = 5000$ episodes to achieve similar performance to the risk-sensitive algorithms in Alg. 5. This indicates better sample efficiency for the proposed risk-sensitive algorithms in Alg. 5. The robustness of the algorithms with respect to model perturbation is further assessed in Fig. 5. Fig. 5a, shows how the $\text{CVaR}_{0.1}$ values decrease as the pole length increases in the risk-neutral case ($\beta = 0$). Fig. 5b and Fig. 5c show that the risk-seeking approaches slightly increase the robustness of the learned policies. However, as shown in Fig. 5d, Fig. 5e, and Fig. 5f, the risk-averse approach ($\beta < 0$) showcases significantly increased robustness with respect to perturbations in the pole length.

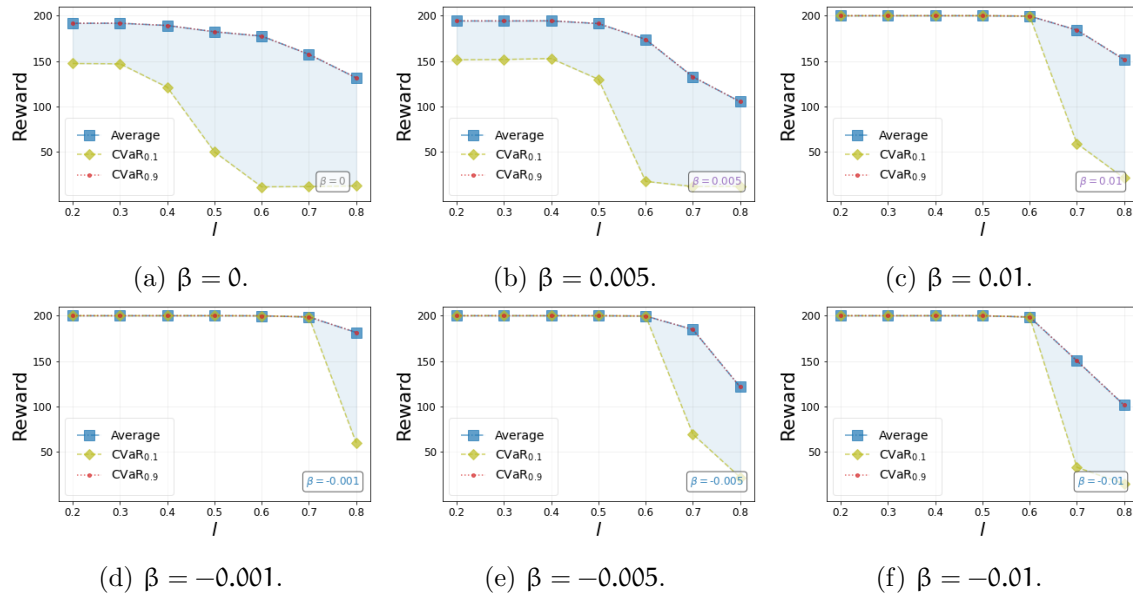


Figure 5: Robustness of risk-neutral Online Actor-Critic (OAC) (Alg. 4) and risk-sensitive R-AC (Alg. 5) algorithms in a cart-pole environment with respect to varying pole length. The training environment is modeled with pole length $l = 0.5$. The testing environments have perturbed pole length values of $l \in [0.2, 0.8]$. Average reward, $\text{CVaR}_{0.1}$, and $\text{CVaR}_{0.9}$ values are computed over 10 independent training and testing runs with different random seeds.

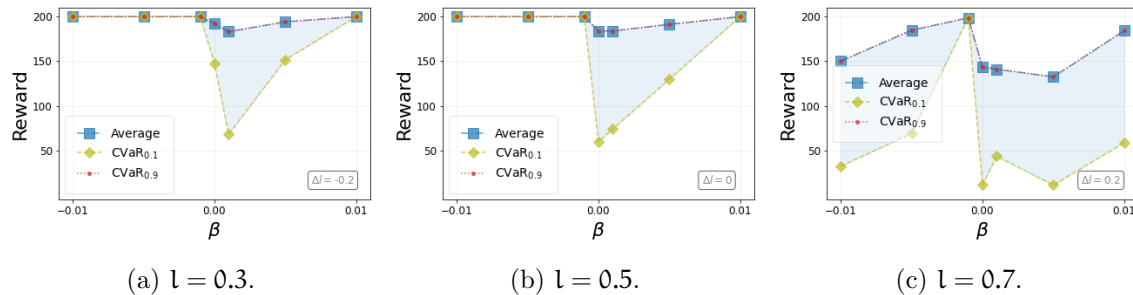


Figure 6: Sensitivity analysis of the risk-sensitive R-AC algorithm (Alg. 5) with respect to the risk-sensitive parameter $\beta \in [-0.01, 0.01]$ in the Cart-Pole problem. $\beta = 0$ corresponds to the risk-neutral Online Actor-Critic (OAC) (Alg. 4). The training environment is modeled with pole length $l = 0.5$. Average reward, $\text{CVaR}_{0.1}$, and $\text{CVaR}_{0.9}$ values for testing environments with $l \in \{0.3, 0.5, 0.7\}$ are computed over 10 independent training and testing runs with different random seeds.

Finally, Fig. 6 presents a sensitivity analysis of the algorithms with respect to the risk-sensitive parameter $\beta \in [-0.01, 0.01]$. Three testing environments are studied for $l = 0.5$ (no perturbation), $l = 0.3$ (overestimation during training), and $l = 0.7$ (underestimation during training). Negative values for β showcase a more stable behavior across the testing

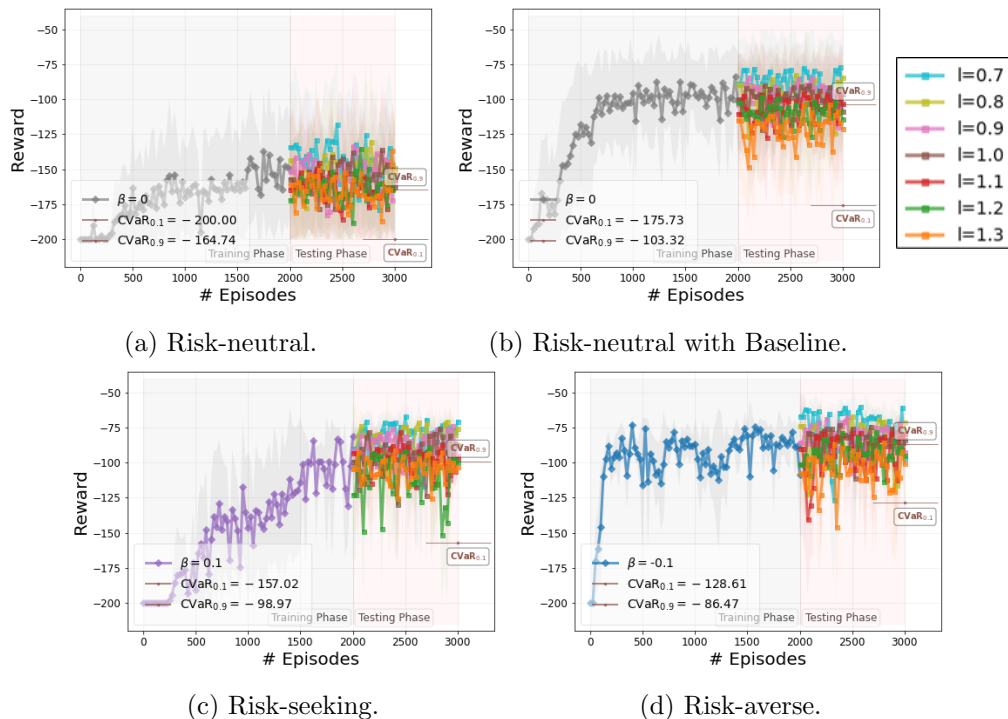


Figure 7: Training and testing behavior of the risk-neutral REINFORCE (Alg. 1) and risk-neutral REINFORCE with baseline (Alg. 2) algorithms against the proposed risk-sensitive R-REINFORCE algorithm (Alg. 3) for $\beta = -0.1$ and $\beta = +0.1$ in the Acrobot problem. Average reward, $\text{CVaR}_{0.1}$, and $\text{CVaR}_{0.9}$ values (for $l = 1.0$) are computed over 10 independent training and testing runs with different random seeds.

environments. Moreover, notice that $\text{sgn}(\beta) < 0$ is roughly adequate for a stable behavior regardless of the numerical value of β , as long as it is close to zero, i.e., no precise estimation of the optimal β is required.

5.3 Underactuated Double Pendulum (Acrobot)

The Acrobot problem is a double pendulum, with the joint between the two pendulum links being actuated and the other joint being un-actuated (Sutton, 1995). The state variable of the acrobot system has six components $(\cos \theta_1, \cos \theta_2, \sin \theta_1, \sin \theta_2, \dot{\theta}_1, \dot{\theta}_2)$, where θ_1 is the angle of the first link with respect to the vertical axis (facing downwards) and θ_2 is the relative angle of the second link with respect to the first link. The action space consists of a torque of $T \in \{-1, 0, +1\}$ Nm of fixed magnitude applied to the actuated joint between the two links. A reward of $r_t = -1$ is given for each time-step that the double pendulum has not reached a given height. Note that the reward structure in Acrobot environment is always negative. An episode is terminated after $N_t = 200$ timesteps that the pendulum has not reached the given height.

In Figure 7 we present the training and testing behavior of the risk-neutral REINFORCE with and without baseline (Alg. 2 and Alg. 1, respectively) algorithms against the proposed

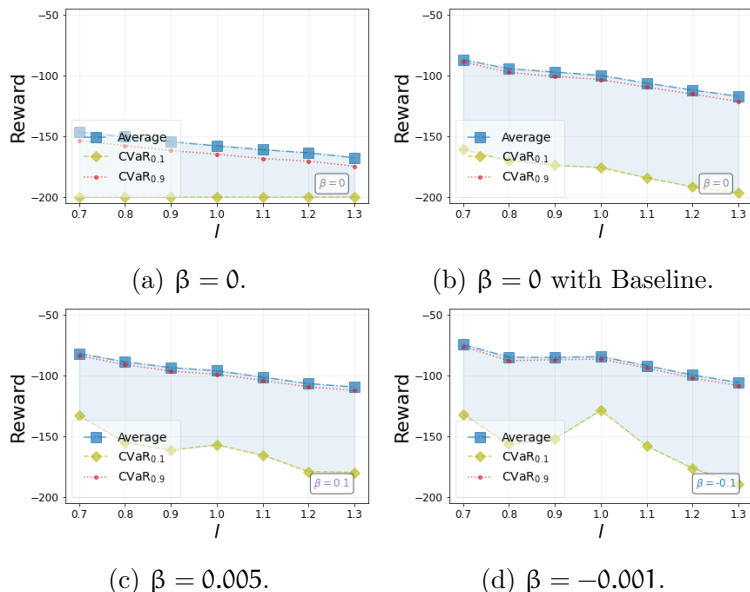


Figure 8: Robustness of risk-neutral REINFORCE (Alg. 1), risk-neutral REINFORCE with baseline (Alg. 2), and risk-sensitive R-REINFORCE (Alg. 3) algorithms in the Acrobot environment with respect to varying pole length. The training environment is modeled with pole length $l = 1.0$. The testing environments have perturbed pole length values of $l \in [0.7, 1.3]$. Average reward, CVaR_{0.1}, and CVaR_{0.9} values are computed over 10 independent training and testing runs with different random seeds.

risk-sensitive R-REINFORCE algorithm (Alg. 3) for $\beta = -0.1$ and $\beta = +0.1$ in the Acrobot problem. The policy networks of the algorithms are modeled as fully connected artificial neural networks with one hidden layer of only $h = 64$ neurons and a ‘ReLU’ activation function. The objective functions to be optimized are as defined in Section 3. We use a discount factor of $\gamma = 0.99$ and the ‘Adam’ optimizer with the best performing learning rates within the set $\{0.001, 0.003, 0.005, 0.007, 0.01\}$ across all algorithms. The algorithms are trained for $n_e = 2000$ episodes in a training environment where the pole length of the first link is $l = 1.0$ and tested in different testing environments for $n_e = 1000$ testing runs where the length of the pole is perturbed such that $l \in [0.7, 1.3]$. The average reward for the different testing environments, as well as the CVaR_{0.1}, and CVaR_{0.9} values for the testing environment without perturbations ($l = 1.0$) are computed over 10 independent training and testing runs with different random seeds.

First, we notice (Fig. 7b) that risk-neutral REINFORCE without baseline is not able to learn a policy that solves the Acrobot problem. On the remaining algorithms, although the mean performance is not significantly different, the risk-sensitive algorithms in Fig. 7d and Fig. 7c showcase increased CVaR_{0.1} values that suggest reduced variation across different runs. The fact that the risk-sensitive approaches perform on par, and slightly better, compared to REINFORCE with baseline, is indicative of the implicit baseline term present in optimizing for the exponential objective function as explained in Section 2.3. The robustness of the algorithms with respect to model perturbation is further assessed in

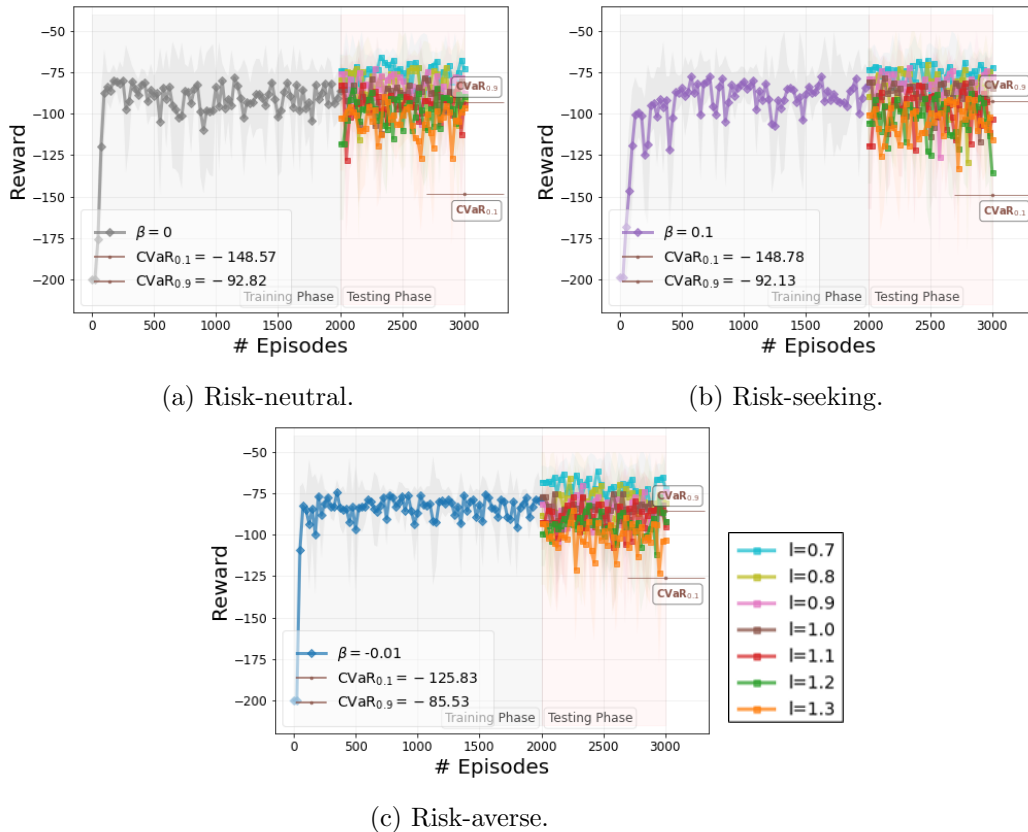


Figure 9: Training and testing behavior of the risk-neutral Online Actor-Critic (OAC) (Alg. 4) algorithm against the proposed risk-sensitive R-AC algorithm (Alg. 5) for $\beta = -0.01$ and $\beta = +0.1$ in the Acrobot problem. Average reward, $\text{CVaR}_{0.1}$, and $\text{CVaR}_{0.9}$ values (for $l = 1.0$) are computed over 10 independent training and testing runs with different random seeds.

Fig. 8 for all testing environments. Similar to the Cart-Pole problem, Fig. 8 suggests that the risk-sensitive approaches can increase the domain of perturbations where the behavior of the RL agent is more stable, with the risk-averse approach ($\beta < 0$) showcasing the best behavior.

Finally, in Figure 9 we present the training and testing behavior of the risk-neutral Online Actor-Critic (OAC) (Alg. 4) and risk-sensitive actor critic (R-AC) (Alg. 5) algorithms in the Acrobot environment with respect to varying pole length. The policy networks of the algorithms are modeled as fully connected artificial neural networks with one hidden layer of only $h = 64$ neurons and a ‘ReLU’ activation function. The objective functions to be optimized are as defined in Section 4.1. We use a discount factor of $\gamma = 0.99$ and the ‘Adam’ optimizer with the best performing learning rates within the set $\{0.0003, 0.0005, 0.0007, 0.001\}$ across all algorithms. The algorithms are trained for $n_e = 2000$ episodes in a training environment where the pole length of the first link is $l = 1.0$ and tested in different testing environments for $n_e = 1000$ testing runs where the length of the pole is perturbed such

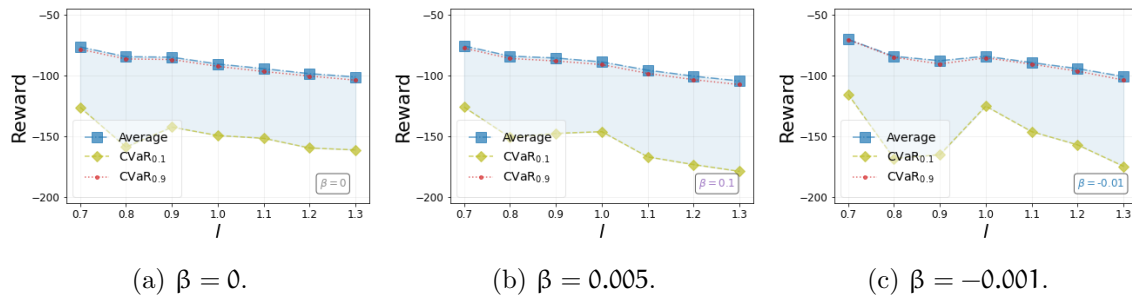


Figure 10: Robustness of risk-neutral Online Actor-Critic (OAC) (Alg. 4) and risk-sensitive R-AC (Alg. 5) algorithms in the Acrobot environment with respect to varying pole length. The training environment is modeled with pole length $l = 1.0$. The testing environments have perturbed pole length values of $l \in [0.7, 1.3]$. Average reward, $\text{CVaR}_{0.1}$, and $\text{CVaR}_{0.9}$ values are computed over 10 independent training and testing runs with different random seeds.

that $l \in [0.7, 1.3]$. The average reward for the different testing environments, as well as the $\text{CVaR}_{0.1}$, and $\text{CVaR}_{0.9}$ values for the testing environment without perturbations ($l = 1.0$) are computed over 10 independent training and testing runs with different random seeds.

Similar to the Cart-Pole case, we notice that although the mean value performance is not significantly different across the three algorithms, the risk-sensitive algorithms in Fig. 9c and Fig. 9b converge to a near-optimal policy that shows reduced variation across different runs, as indicated by the $\text{CVaR}_{0.1}$, and $\text{CVaR}_{0.9}$ values calculated for $l = 1.0$ (no model perturbations). The robustness of the algorithms with respect to model perturbation is further assessed in Fig. 10. Fig. 10a, shows how the $\text{CVaR}_{0.1}$ values decrease as the pole length increases in the risk-neutral case ($\beta = 0$). Fig. 10c shows that the risk-averse approach can increase the robustness of the learned policies for small perturbations.

These results are consistent with the analysis presented in Section 2 and suggest that the use of exponential criteria results in a risk-sensitive reinforcement learning approach that inherit computational and convergence properties of standard RL algorithms, but can also further accelerate the learning process, leading in increased sample efficiency, and result in policies with increased robustness with respect to environmental and model perturbations.

6. Conclusion

Risk-sensitive reinforcement learning algorithms are receiving increasing attention in an endeavor to construct robust and sample-efficient algorithms which can lead to increased performance compared to their risk-neutral counterparts. We formulate a risk-sensitive reinforcement learning approach as an optimization problem with respect to a modified objective based on exponential criteria. In particular, we study a model-free risk-sensitive variation of the widely-used Monte Carlo Policy Gradient algorithm, and introduce a novel risk-sensitive online Actor-Critic algorithm based on solving a multiplicative Bellman equation using stochastic approximation updates. Analytical results suggest that the use of exponential criteria generalizes commonly used ad-hoc regularization approaches, improves sample efficiency, and introduces robustness with respect to perturbations in the model

parameters and the environment. The implementation, performance, and robustness properties of the proposed methods are evaluated in simulated experiments, and suggest suitability for real-life applications where learning in simulation is followed by transferring the learned policies to real agents in noisy environments.

Acknowledgments

This work was supported in part by US Office of Naval Research (ONR) Grant No. N00014-17-1-2622, by US NSF Grant ECCS2127605, by the Clark Foundation Distinguished Fellowship, and by the University of Maryland Graduate School Ann G. Wylie Fellowship.

Appendix A. Risk-Sensitive Policy Gradient Update Rule

In this section, we provide a risk-sensitive version of the policy gradient theorem (Sutton et al., 1999) using exponential criteria, which is used to derive the update rule for the Risk-Sensitive REINFORCE algorithm in (26). Using the definition of expectation, the exponential objective can be written as an integral (summation for finite state and action spaces) over all possible trajectories, i.e.,

$$\begin{aligned}
 \nabla_{\theta} J_{\beta}(\theta) &= \nabla \frac{1}{\beta} \int \rho_{\theta}(\tau) \exp\{\beta R(\tau)\} d\tau \\
 &= \frac{1}{\beta} \int \nabla \rho_{\theta}(\tau) \exp\{\beta R(\tau)\} d\tau \\
 &= \frac{1}{\beta} \int \rho_{\theta}(\tau) \frac{\nabla \rho_{\theta}(\tau)}{\rho_{\theta}(\tau)} \exp\{\beta R(\tau)\} d\tau \\
 &= \frac{1}{\beta} \int \rho_{\theta}(\tau) \nabla \log \rho_{\theta}(\tau) \exp\{\beta R(\tau)\} d\tau \\
 &= \frac{1}{\beta} \mathbb{E}_{\tau \sim \rho_{\theta}} \left[\nabla \log \rho_{\theta}(\tau) \exp\{\beta R(\tau)\} \right]
 \end{aligned} \tag{42}$$

Using the “log-trick” (Sutton & Barto, 2018), the gradient of the $J_{\beta}(\theta)$ with respect to the policy parameter θ can be obtained as follows,

$$\begin{aligned}
 \nabla_{\theta} J_{\beta}(\theta) &= \nabla \frac{1}{\beta} \int \rho_{\theta}(\tau) \exp\{\beta R(\tau)\} d\tau \\
 &= \frac{1}{\beta} \mathbb{E}_{\tau \sim \rho_{\theta}} \left[\nabla \log \rho_{\theta}(\tau) \exp\{\beta R(\tau)\} \right]
 \end{aligned} \tag{43}$$

Recall that $\rho_{\theta}(\tau) = p_0 \prod_{t=0}^{|\tau|-1} \pi(\mathbf{a}_t | \mathbf{s}_t; \theta) p(\mathbf{s}_{t+1} | \mathbf{s}_t, \mathbf{a}_t)$. Then, by first taking the logarithm and then the gradient of both sides, we get

$$\nabla \log \rho_{\theta}(\tau) = \sum_{t=0}^{|\tau|-1} \nabla \log \pi(\mathbf{a}_t | \mathbf{s}_t; \theta) \tag{44}$$

For brevity, we use $\pi_t(\theta) := \pi(\mathbf{a}_t | \mathbf{s}_t; \theta)$. Thus, by substituting Eq. (44) in Eq. (42), we get

$$\nabla J_\theta(\theta) = \frac{1}{\beta} \mathbb{E}_{\tau \sim \rho_\theta} \left[\sum_{t=0}^{|\tau|-1} \nabla \log \pi_t(\theta) \exp\{\beta R(\tau)\} \right] \quad (45)$$

Recall that $R(\tau) = \sum_{t=0}^{|\tau|-1} \gamma^t r(\mathbf{s}_t, \mathbf{a}_t)$. Using this fact and the property of exponential, we have

$$\nabla J_\theta(\theta) = \frac{1}{\beta} \mathbb{E}_{\tau \sim \rho_\theta} \left[\sum_{t=0}^{|\tau|-1} \nabla \log \pi_t(\theta) \exp\left\{\beta \sum_{t'=0}^{t-1} \gamma^{t'} r(\mathbf{s}_{t'}, \mathbf{a}_{t'})\right\} \exp\left\{\beta \sum_{t'=t}^{|\tau|-1} \gamma^{t'} r(\mathbf{s}_{t'}, \mathbf{a}_{t'})\right\} \right] \quad (46)$$

By using the temporal structure of the problem and causality, it can be argued that the rewards prior to time t are not dependent on the actions that the policy will take in a future state \mathbf{s}_t , that is, $\sum_{t'=0}^{t-1} \gamma^{t'} r(\mathbf{s}_{t'}, \mathbf{a}_{t'})$ is independent of $\nabla \log \pi(\mathbf{a}_t | \mathbf{s}_t; \theta)$. Thus, by using the independence property, we have

$$\nabla J_\theta(\theta) = \frac{1}{\beta} \mathbb{E}_{\tau \sim \rho_\theta} \left[\exp\left\{\beta \sum_{t'=0}^{t-1} \gamma^{t'} r(\mathbf{s}_{t'}, \mathbf{a}_{t'})\right\} \right] \mathbb{E}_{\tau \sim \rho_\theta} \left[\sum_{t=0}^{|\tau|-1} \nabla \log \pi_t(\theta) \exp\left\{\beta \sum_{t'=t}^{|\tau|-1} \gamma^{t'} r(\mathbf{s}_{t'}, \mathbf{a}_{t'})\right\} \right] \quad (47)$$

Note that the first expectation is a constant, therefore,

$$\nabla J_\theta(\theta) \propto \mathbb{E}_{\tau \sim \rho_\theta} \left[\sum_{t=0}^{|\tau|-1} \frac{1}{\beta} e^{\beta R_t} \nabla \log \pi_t(\theta) \right] \quad (48)$$

where $R_t := \sum_{t'=t}^{|\tau|-1} \gamma^{t'-t} r(\mathbf{s}_{t'}, \mathbf{a}_{t'})$.

As a final remark, notice that from (47), we can see that the first term on the right hand side of the equation provides an inherent way of adjusting the step size, effectively making the constant step size adaptive.

A.1 Convergence Analysis

In this section we show that the the parameter vector θ updated by the risk-sensitive REINFORCE algorithm in (26) converges to the optimal parameter vector θ^* in expectation, for sufficiently small values of the risk-parameter β . First note the following identity

$$\begin{aligned} \|\theta_{t+1} - \theta^*\|^2 - \|\theta_t - \theta^*\|^2 &= \|\theta_{t+1} - \theta_t + \theta_t - \theta^*\|^2 - \|\theta_t - \theta^*\|^2 \\ &= \|\theta_{t+1} - \theta_t\|^2 - 2(\theta_{t+1} - \theta_t) \cdot (\theta_t - \theta^*) \end{aligned}$$

Using the R-REINFORCE update rule in (26), i.e.,

$$\theta_{t+1} = \theta_t + \frac{\eta}{\beta} e^{\beta R_t^+} \nabla \log \pi_{\theta_t}(\mathbf{a}_t | \mathbf{s}_t)$$

we get

$$\begin{aligned} \|\theta_{t+1} - \theta^*\|^2 - \|\theta_t - \theta^*\|^2 &= \left(\frac{\eta}{\beta} e^{\beta R_t^+}\right)^2 \|\nabla \log \pi_{\theta_t}(\mathbf{a}_t | \mathbf{s}_t)\|^2 \\ &\quad - 2 \frac{\eta}{\beta} e^{\beta R_t^+} \nabla \log \pi_{\theta_t}(\mathbf{a}_t | \mathbf{s}_t) \cdot (\theta_t - \theta^*) \end{aligned}$$

By taking the conditional expectation with filtration \mathcal{F}_t from both sides of the equation, we have

$$\begin{aligned} \mathbb{E}\left[\|\theta_{t+1} - \theta^*\|^2 \mid \mathcal{F}_t\right] &= \|\theta_t - \theta^*\|^2 + \left(\frac{\eta}{\beta}\right)^2 \mathbb{E}\left[e^{2\beta R_t^+} \|\nabla \log \pi_{\theta_t}(\mathbf{a}_t | \mathbf{s}_t)\|^2 \mid \mathcal{F}_t\right] \\ &\quad - 2\frac{\eta}{\beta} e^{-\beta R_t^-} \mathbb{E}\left[e^{\beta R_t} \nabla \log \pi_{\theta_t}(\mathbf{a}_t | \mathbf{s}_t) \mid \mathcal{F}_t\right] \cdot (\theta_t - \theta^*) \\ &= \|\theta_t - \theta^*\|^2 + \left(\frac{\eta}{\beta}\right)^2 \mathbb{E}\left[e^{2\beta R_t^+} \|\nabla \log \pi_{\theta_t}(\mathbf{a}_t | \mathbf{s}_t)\|^2 \mid \mathcal{F}_t\right] \\ &\quad - 2\eta e^{-\beta R_t^-} \nabla J_\gamma(\theta_t) \cdot (\theta_t - \theta^*) \end{aligned}$$

The first line follows from the conditioning on the filtration \mathcal{F}_t . The second line follows from the fact that $\nabla J_\gamma(\theta_t) = \mathbb{E}\left[\frac{1}{\beta} e^{\beta R_t} \nabla \log \pi_{\theta_t}(\mathbf{a}_t | \mathbf{s}_t) \mid \mathcal{F}_t\right]$. It should be noted that since $\theta^* = \operatorname{argmax}_\theta J_\gamma(\theta)$, it follows that $\nabla J_\gamma(\theta_t) \cdot (\theta_t - \theta^*) > 0$. Finally, it follows that θ_t converges to θ^* , as long as the following condition holds:

$$\left(\frac{\eta}{\beta}\right)^2 \mathbb{E}\left[e^{2\beta R_t^+} \|\nabla \log \pi_{\theta_t}(\mathbf{a}_t | \mathbf{s}_t)\|^2 \mid \mathcal{F}_t\right] - 2\eta e^{-\beta R_t^-} \nabla J_\gamma(\theta_t) \cdot (\theta_t - \theta^*) < 0.$$

References

- Abdolmaleki, A., Springenberg, J. T., Tassa, Y., Munos, R., Heess, N., & Riedmiller, M. (2018). Maximum a posteriori policy optimisation..
- Abdullah, M. A., Ren, H., Ammar, H. B., Milenkovic, V., Luo, R., Zhang, M., & Wang, J. (2019). Wasserstein robust reinforcement learning..
- Barto, A. G., Sutton, R. S., & Anderson, C. W. (1983). Neuronlike adaptive elements that can solve difficult learning control problems. *IEEE transactions on systems, man, and cybernetics*, *SMC-13*(5), 834–846.
- Basar, T., & Bernhard, P. (2008). *H-infinity Optimal Control and Related Minimax Design Problems: A Dynamic Game Approach*. Springer Science & Business Media.
- Bhatnagar, S., Sutton, R. S., Ghavamzadeh, M., & Lee, M. (2009). Natural actor–critic algorithms. *Automatica*, *45*(11), 2471 – 2482.
- Borkar, V. S. (2002). Q-learning for risk-sensitive control. *Mathematics of operations research*, *27*(2), 294–311.
- Borkar, V. S. (2009). *Stochastic approximation: a dynamical systems viewpoint*, Vol. 48. Springer.
- Borkar, V. S. (2010). Learning algorithms for risk-sensitive control. *Proceedings of the 19th International Symposium on Mathematical Theory of Networks and Systems*, 5(9).
- Chow, Y., & Ghavamzadeh, M. (2014). Algorithms for CVaR Optimization in MDPs. *Advances in Neural Information Processing Systems*, *27*, 3509–3517.
- Dai Pra, P., Meneghini, L., & Runggaldier, W. J. (1996). Connections between stochastic control and dynamic games. *Mathematics of Control, Signals and Systems*, *9*(4), 303–326.

- Delage, E., & Mannor, S. (2010). Percentile optimization for markov decision processes with parameter uncertainty. *Operations research*, 58(1), 203–213.
- Dotan Di Castro, A. T., & Mannor, S. (2012). Policy Gradients with Variance Related Risk Criteria. In *Proceedings of the 29th International Conference on Machine Learning, Edinburgh, Scotland, UK*.
- Eysenbach, B., & Levine, S. (2021). Maximum entropy rl (provably) solves some robust rl problems..
- Fei, Y., Yang, Z., Chen, Y., & Wang, Z. (2021). Exponential bellman equation and improved regret bounds for risk-sensitive reinforcement learning. *Advances in Neural Information Processing Systems*, 34.
- Fei, Y., Yang, Z., Chen, Y., Wang, Z., & Xie, Q. (2020). Risk-sensitive reinforcement learning: Near-optimal risk-sample tradeoff in regret. *Advances in Neural Information Processing Systems*, 33, 22384–22395.
- Föllmer, H., & Schied, A. (2002). Convex Measures of Risk and Trading Constraints. *Finance and stochastics*, 6(4), 429–447.
- Galashov, A., Jayakumar, S. M., Hasenclever, L., Tirumala, D., Schwarz, J., Desjardins, G., Czarnecki, W. M., Teh, Y. W., Pascanu, R., & Heess, N. M. O. (2019). Information Asymmetry in KL-regularized RL. *ArXiv, abs/1905.01240*.
- Grathwohl, W., Choi, D., Wu, Y., Roeder, G., & Duvenaud, D. (2017). Backpropagation Through The Void: Optimizing Control Variates for Black-box Gradient Estimation..
- Greenberg, I., Chow, Y., Ghavamzadeh, M., & Mannor, S. (2022). Efficient risk-averse reinforcement learning. *Advances in Neural Information Processing Systems*, 35, 32639–32652.
- Gu, S., Lillicrap, T., Sutskever, I., & Levine, S. (2016). Continuous deep q-learning with model-based acceleration. In *International Conference on Machine Learning*, pp. 2829–2838. PMLR.
- Gu, S. S., Lillicrap, T., Turner, R. E., Ghahramani, Z., Schölkopf, B., & Levine, S. (2017). Interpolated Policy Gradient: Merging On-policy and Off-policy Gradient Estimation for Deep Reinforcement Learning. In *Advances in Neural Information Processing Systems*, pp. 3846–3855.
- Haarnoja, T., Tang, H., Abbeel, P., & Levine, S. (2017). Reinforcement Learning with Deep Energy-Based Policies. In *Proceedings of the 34th International Conference on Machine Learning - Volume 70, ICML’17*, p. 1352–1361. JMLR.org.
- Haarnoja, T., Zhou, A., Abbeel, P., & Levine, S. (2018). Soft Actor-Critic: Off-Policy Maximum Entropy Deep Reinforcement Learning with a Stochastic Actor. In Dy, J., & Krause, A. (Eds.), *Proceedings of the 35th International Conference on Machine Learning*, Vol. 80 of *Proceedings of Machine Learning Research*, pp. 1861–1870, Stockholmsmässan, Stockholm Sweden. PMLR.
- Hansen, L. P., & Sargent, T. J. (2011). Robustness. In *Robustness*. Princeton university press.

- Jacobson, D. (1973). Optimal Stochastic Linear Systems with Exponential Performance Criteria and Their Relation to Deterministic Differential Games. *IEEE Transactions on Automatic Control*, 18(2), 124–131.
- James, M. R., & Baras, J. S. (1995). Robust H_∞ output feedback control for nonlinear systems. *IEEE Transactions on Automatic Control*, 40(6), 1007–1017.
- Kakade, S. M. (2001). A Natural Policy Gradient. *Advances in Neural Information Processing Systems*, 14, 1531–1538.
- Konda, V., & Tsitsiklis, J. (1999). Actor-critic algorithms. *Advances in neural information processing systems*, 12.
- Konda, V. R., & Tsitsiklis, J. N. (2003). On Actor-Critic Algorithms. *SIAM J. Control Optim.*, 42(4), 1143–1166.
- La, P., & Ghavamzadeh, M. (2013). Actor-critic algorithms for risk-sensitive mdps. *Advances in neural information processing systems*, 26.
- Lewis, F. L., Vrabie, D., & Vamvoudakis, K. G. (2012). Reinforcement learning and feedback control: Using natural decision methods to design optimal adaptive controllers. *IEEE Control Systems Magazine*, 32(6), 76–105.
- Liu, B., Liu, J., & Xiao, K. (2018). R2PG: Risk-Sensitive and Reliable Policy Gradient. In *The Workshops of the The Thirty-Second AAAI Conference on Artificial Intelligence, New Orleans, Louisiana, USA, February 2-7, 2018*, Vol. WS-18 of *AAAI Workshops*, pp. 682–687. AAAI Press.
- Liu, H., Feng, Y., Mao, Y., Zhou, D., Peng, J., & Liu, Q. (2017). Action-depedent Control Variates for Policy Optimization via Stein’s Identity..
- Mavridis, C., Noorani, E., & Baras, J. S. (2022). Risk sensitivity and entropy regularization in prototype-based learning. In *2022 30th Mediterranean Conference on Control and Automation (MED)*, pp. 194–199. IEEE.
- Mavridis, C. N., & Baras, J. S. (2021). Vector quantization for adaptive state aggregation in reinforcement learning. In *2021 American Control Conference (ACC)*, pp. 2187–2192. IEEE.
- Mavridis, C. N., & Baras, J. S. (2022). Annealing optimization for progressive learning with stochastic approximation. *IEEE Transactions on Automatic Control*, 70, 1–13.
- Mavridis, C. N., Suriyarachchi, N., & Baras, J. S. (2021). Maximum-entropy progressive state aggregation for reinforcement learning. In *2021 60th IEEE Conference on Decision and Control (CDC)*, pp. 5144–5149. IEEE.
- Moos, J., Hansel, K., Abdulsamad, H., Stark, S., Clever, D., & Peters, J. (2022). Robust reinforcement learning: A review of foundations and recent advances. *Machine Learning and Knowledge Extraction*, 4(1), 276–315.
- Nass, D., Belousov, B., & Peters, J. (2019). Entropic Risk Measure in Policy Search. In *2019 IEEE/RSJ International Conference on Intelligent Robots and Systems (IROS)*, pp. 1101–1106.

- Noorani, E., & Baras, J. S. (2021a). Risk-sensitive reinforce: A monte carlo policy gradient algorithm for exponential performance criteria. In *2021 60th IEEE Conference on Decision and Control (CDC)*, pp. 1522–1527. IEEE.
- Noorani, E., & Baras, J. S. (2021b). Risk-sensitive reinforcement learning and robust learning for control. In *2021 60th IEEE Conference on Decision and Control (CDC)*, pp. 2976–2981. IEEE.
- Noorani, E., & Baras, J. S. (2022). Embracing risk in reinforcement learning: The connection between risk-sensitive exponential and distributionally robust criteria. In *2022 American Control Conference (ACC)*, pp. 2703–2708.
- Osogami, T. (2012). Robustness and risk-sensitivity in markov decision processes. *Advances in Neural Information Processing Systems*, 25.
- Pan, X., Seita, D., Gao, Y., & Canny, J. (2019). Risk averse robust adversarial reinforcement learning. In *2019 International Conference on Robotics and Automation (ICRA)*, pp. 8522–8528. IEEE.
- Paternain, S., Chamon, L., Calvo-Fullana, M., & Ribeiro, A. (2019). Constrained reinforcement learning has zero duality gap. *Advances in Neural Information Processing Systems*, 32.
- Pinto, L., Davidson, J., Sukthankar, R., & Gupta, A. (2017). Robust Adversarial Reinforcement Learning. In *International Conference on Machine Learning*, pp. 2817–2826. PMLR.
- Prashanth, L. A. (2014). Policy gradients for cvar-constrained mdps. In Auer, P., Clark, A., Zeugmann, T., & Zilles, S. (Eds.), *Algorithmic Learning Theory*, pp. 155–169, Cham. Springer International Publishing.
- Reddy, D. S. K., Saha, A., Tamilselvam, S. G., Agrawal, P., & Dayama, P. (2019). Risk averse reinforcement learning for mixed multi-agent environments. In *Proceedings of the 18th international conference on autonomous agents and multiagent systems*, pp. 2171–2173.
- Scarf, H. E. (1957). *A min-max solution of an inventory problem*. Rand Corporation Santa Monica.
- Schulman, J., Levine, S., Abbeel, P., Jordan, M., & Moritz, P. (2015). Trust Region Policy Optimization. In Bach, F., & Blei, D. (Eds.), *Proceedings of the 32nd International Conference on Machine Learning*, Vol. 37 of *Proceedings of Machine Learning Research*, pp. 1889–1897, Lille, France. PMLR.
- Schulman, J., Wolski, F., Dhariwal, P., Radford, A., & Klimov, O. (2017). Proximal Policy Optimization Algorithms..
- Shapley, L. S. (1953). Stochastic games. *Proceedings of the national academy of sciences*, 39(10), 1095–1100.
- Sutton, R. S. (1995). Generalization in reinforcement learning: Successful examples using sparse coarse coding. *Advances in neural information processing systems*, 8.
- Sutton, R. S., & Barto, A. G. (2018). *Reinforcement learning: An introduction*. MIT press.

- Sutton, R. S., McAllester, D., Singh, S., & Mansour, Y. (1999). Policy gradient methods for reinforcement learning with function approximation. *Advances in neural information processing systems*, 12.
- Sutton, R. S., McAllester, D. A., Singh, S. P., & Mansour, Y. (2000). Policy Gradient Methods for Reinforcement Learning With Function Approximation. In *Advances in Neural Information Processing Systems*, pp. 1057–1063.
- Tamar, A. (2015). Risk-Sensitive and Efficient Reinforcement Learning Algorithms..
- Tamar, A., Xu, H., & Mannor, S. (2013). Scaling up robust mdps by reinforcement learning..
- Thomas, P. S., & Brunskill, E. (2017). Policy Gradient Methods for Reinforcement Learning with Function Approximation and Action-dependent Baselines..
- Todorov, E. (2007). Linearly-solvable Markov Decision Problems. In *Advances in Neural Information Processing Systems*, pp. 1369–1376.
- Tsitsiklis, J. N., & Van Roy, B. (1997). An analysis of temporal-difference learning with function approximation. *IEEE Transactions on Automatic Control*, 42(5), 674–690.
- Tucker, G., Bhupatiraju, S., Gu, S., Turner, R., Ghahramani, Z., & Levine, S. (2018). The Mirage of Action-Dependent Baselines in Reinforcement Learning. In Dy, J., & Krause, A. (Eds.), *Proceedings of the 35th International Conference on Machine Learning*, Vol. 80 of *Proceedings of Machine Learning Research*, pp. 5015–5024, Stockholm, Stockholm, Stockholm Sweden. PMLR.
- Weaver, L., & Tao, N. (2013). The optimal reward baseline for gradient-based reinforcement learning..
- Williams, R. J. (1992). Simple statistical gradient-following algorithms for connectionist reinforcement learning. *Machine learning*, 8(3), 229–256.
- Williams, R. J., & Peng, J. (1991). Function Optimization Using Connectionist Reinforcement Learning Algorithms. *Connection Science*, 3(3), 241–268.
- Wu, C., Rajeswaran, A., Duan, Y., Kumar, V., Bayen, A. M., Kakade, S., Mordatch, I., & Abbeel, P. (2018). Variance Reduction for Policy Gradient with Action-dependent Factorized Baselines..
- Ziebart, B. D., Maas, A., Bagnell, J. A., & Dey, A. K. (2008). Maximum Entropy Inverse Reinforcement Learning. In *Proceedings of the 23rd National Conference on Artificial Intelligence - Volume 3*, AAAI’08, p. 1433–1438. AAAI Press.